fected young and adult mice were compared, the adult animals had significantly lower pre-existing lymphocyte and $CD4^+$ and $CD8^+$ T-cell counts, their lungs expressed significantly higher IL-4 and lower IL-10 and IL-13 levels before infection, and their lungs did not show the strong up-regulation of IL-2 (a T-cell cytokine), IL-10, IL-13, and IFN-γ that was exhibited by the young murine lungs after infection. During the infection, the lungs of adult mice also produced inflammatory chemokine-/cytokine-related macrophages (ie, MCP-1, MIP-1 and IP-10, IL-1α, IL-1β, and TNF-α) earlier than young mice (day 1 after inoculation) and at higher levels. They also had higher IL-6 levels on day 3 after inoculation. In contrast, the young mice produced high levels of inflammatory chemokines and cytokines (ie, MCP-1, MIP-1, IP-10, KC, MIG, VEGF, and IL-1α) on day 2 after inoculation and produced very little IL-6 at any time point. These observations suggest that advanced-age BALB/c mice have an early and acutely excessive proinflammatory cytokine reactions (ie, a cytokine storm) in response to F-musX-VeroE6. This cytokine storm results in severe pulmonary edema with macrophage and neutrophil infiltration, which causes severe acute lung injury and is likely to be the cause of death in infected adult mice. Supporting this scenario are reports of age-related differences in pulmonary cytokine and chemokine responses to other pathogens, especially Th1 and Th2 cytokine imbalances.[31–33]

Moreover, recent reports showed that unregulated IFN responses during acute SARS prevented SARS-CoV-infected patients from switching from innate to adaptive immunity,[39,40] and some reports described that IFN-γ may be responsible for lung immunopathology in SARS patients.[41,42] Interestingly, in our model, injection of IFN-γ 3 hours after inoculation significantly reduced the acute pulmonary edema induced by infection. Notably, these protective effects of IFN-γ injection were not associated with reductions in viral titers in the lung. This animal model and human results seem not to be consistent. However, these observations together suggest that the failure of the adult animals to produce IFN-γ, which is a prominent immunomodulator that plays a key role in host defense against intracellular pathogens,[43,44] was responsible for their inability to control the excessive and pathogenic innate immune response to the virus in the lung. Supporting this is our previous study on the rat SARS model, which showed that although adult rats developed severe inflammatory reactions that led to pulmonary edema, all of the infected animals survived; significantly, the infected adult rats had similar cytokine profiles as infected adult mice except that they also produced IFN-γ.[34] Thus, a strong and timely IFN-γ response may be needed to prevent the immunopathology induced by SARS-CoV infection.

With regard to the inflammatory reactions in the F-musX-VeroE6-infected adult lung, our histopathological and chemokine/cytokine analyses suggested that on day 1 after inoculation, the affected respiratory epithelial cells and pulmonary macrophages released acute inflammatory chemokines (MCP-1, MIP-1, IP-10) and cytokines (IL-1, TNF-α, IL-12). Thus, pulmonary macrophage activation associated with the release of TNF-α and IL-1 appears to predominate in the early phase of the inflammatory reaction in adults. TNF-α and IL-1 are classic acute inflammatory cytokines that recruit neutrophils and monocytes to the area of infection along with increasing vascular permeability, where they activate these cells so that they can eradicate the pathogens. However, when TNF-α is overexpressed, it can induce systemic clinical and pathological abnormalities such as depressing cardiac dysfunction and cardiomyocyte death.[45,46] This double-edged aspect of TNF-α function may be why there were no effects of neutralizing TNF-α antibodies on SARS-CoV infection in this model. Supporting the key role of TNF-α in F-musX-VeroE6-induced immunopathology is that the lungs of the adult mice on days 3 and 5 after inoculation were infiltrated with predominantly neutrophils; these mice also exhibited neutrophilia. Young mice did not evince these changes. This suggested that infected adult mice produce TNF-α, which then induces neutrophil-mediated inflammation in their lungs. Although the significance of this is not clear, high neutrophil infiltration in the lung is known to be the cause or the result of lung injury characterized by hyaline membrane formation and pulmonary edema.[47] High neutrophil counts in human SARS cases have also been associated with poor outcomes.[8,10]

We observed in the anti-TNF-α antibody and IFN-γ-injection experiments that the control groups, which were injected 3 hours after infection with rat IgG serum intravenously or PBS intraperitoneally, showed body weight loss starting on day 1 after inoculation. In contrast, untreated mice (such as those shown in Figures 1F and 2A) only started to lose weight on day 2 after inoculation. It may be that the injection with serum or PBS after the infection enhanced the pulmonary edema by hyperpermeability in the lung.

We previously reported that serial *in vivo* passage of SARS-CoV in F344 rats increased the infectivity of the virus in rats, and that this correlated with a single amino acid change in the virus receptor-binding domain of the S protein.[34] We detected the similar change in F-musX-VeroE6 along with another amino acid change in the receptor-binding domain of the S protein in F-musX-VeroE6. The amino acid change may be responsible, at least in part, for the increased replication of F-musX-VeroE6 in the pulmonary tissue of BALB/c mice.[12–15,34,48] Using another SARS-CoV isolate (Urbani), Roberts and colleagues[48] have described the development and characterization of the mouse-adapted strain MA15, which is lethal for young (6- to 8-week-old) female BALB/c mice after intranasal inoculation. Compared with the original Urbani isolate, the MA15 strain had six coding mutations that may have been responsible for the mouse adaptation and increased virulence of this strain. The fewer amino acid mutations in our mouse-adapted F-musX-VeroE6 strain may be responsible for the fact that it is less virulent than MA15.

In conclusion, we developed an experimental mouse animal model of SARS by using *in vivo*-passaged SARS-CoV and BALB/c mice. We found that the virus was lethal in adult mice because they generated an excessive innate immune response that induced lethal pulmonary

edema and diffuse alveolar damage with infiltration of macrophages and neutrophils. IFN-γ appears to play an important role in modulating the innate immune response because IFN-γ treatment protected the animals from the lethal respiratory illness. This study, along with our previous study[34] and studies of humans infected with SARS-CoV during the SARS epidemic of winter of 2002 to 2003,[6–10] improve our understanding of SARS pathogenesis because they indicate that both advanced age and virus adaptation to a particular animal species may dictate the pathogenic capacity of SARS-CoV. The new experimental model described here may also be useful for elucidating the pathophysiology of SARS and for evaluating anti-SARS-CoV vaccine candidates and antiviral agents.

Acknowledgments

We thank Dr. John Ziebuhr for kindly supplying the Frankfurt 1 isolate; the colleagues of our institute, especially Ms. Mihoko Fujino, Ms. Michiyo Kataoka, and Mr. Ikuyoshi Hatano, for their technical assistance; Dr. Yasuko Tsunetsugu-Yokota and Dr. Yasushi Ami for valuable discussions; Dr. Rie Watanabe and Dr. Kazuya Shirato for their technical expertise in virus genome sequencing; Dr. Noriko Nakajima for her technical expertise in confocal laser-scanning microscopy and valuable discussions; and Dr. Yoshinobu Horiuchi and Dr. Masaki Ochiai for their technical experts in the LPS kinetic chromatogenic assay and valuable discussions.

References

1. Drosten C, Günther S, Preiser W, van der Werf S, Brodt HR, Becker S, Rabenau H, Panning M, Kolesnikova L, Fouchier RAM, Berger A, Burguière AM, Cinatl J, Eickmann M, Escriou N, Grywna K, Kramme S, Mariuguerra JC, Müller S, Rickerts V, Stürmer M, Vieth S, Klenk HD, Osterhaus ADME, Schmitz H, Doerr HW: Identification of a novel coronavirus in patients with severe acute respiratory syndrome. N Engl J Med 2003, 348:1967–1976
2. Fouchier RAM, Kuiken T, Schutten M, van Amerongen G, van Doornum GJJ, van den Hoogen BG, Peiris M, Lim W, Stöhr K, Osterhaus ADME: Koch's postulates fulfilled for SARS virus. Nature 2003, 423:240
3. Ksiazek TG, Erdman D, Goldsmith CS, Zaki SR, Peret T, Emery S, Tong S, Urbani C, Comer JA, Lim W, Rollin PE, Dowell SF, Ling AE, Humphrey CD, Shieh WJ, Guarner J, Paddock CD, Rota MPHTMP, Fields B, DeRisi J, Yang JY, Cox N, Hughes JM, LeDuc JW, Bellini WJ, Anderson LJ, the SARS Working Group: A novel coronavirus associated with severe acute respiratory syndrome. N Engl J Med 2003, 348:1953–1966
4. Kuiken T, Fouchier RAM, Schutten M, Rimmelzwaan GF, van Amerongen G, van Riel D, Laman JD, de Jong T, van Doornum G, Lim W, Ling AE, Chan PKS, Tam JS, Zambon MC, Gopal R, Drosten C, van der Werf S, Escriou N, Manuguerra JC, Stöhr K, Peiris JSM, Osterhaus ADME: Newly discovered coronavirus as the primary cause of severe acute respiratory syndrome. Lancet 2003, 362:263–270
5. Peiris JSM, Lai ST, Poon LLM, Guan Y, Yam LYC, Lim W, Nicholls J, Yee WKS, Yan WW, Cheung MT, Cheng VCC, Chan KH, Tsang DNC, Yung RWH, Ng TK, Yuen KY, members of the SARS Study Group: Coronavirus as a possible cause of severe acute respiratory syndrome. Lancet 2003, 361:1319–1325
6. Booth CM, Matukas LM, Tomlinson GA, Rachlis AR, Rose DB, Dwosh HA, Walmsley SL, Mazzulli T, Avendano M, Derkach P, Ephtimios IE, Kitai I, Mederski BD, Shadowitz SB, Gold WL, Hawryluck LA, Rea E, Chenkin JS, Cescon DW, Poutanen SM, Detsky AS: Clinical features and short-term outcomes of 144 patients with SARS in the greater Toronto area. JAMA 2003, 289:2801–2809
7. Donnelly CA, Ghani AC, Leung GM, Hedley AJ, Fraser C, Riley S, Abu-Raddad LJ, Ho LM, Thach TQ, Chau P, Chan KP, Lam TH, Tse LY, Tsang T, Liu SH, Kong JH, Lau EM, Ferguson NM, Anderson RM: Epidemiological determinants of spread of causal agent of severe acute respiratory syndrome in Hong Kong. Lancet 2003, 361:1761–1766
8. Lee N, Hui D, Wu A, Chan P, Cameron P, Joynt GM, Ahuja A, Yung MY, Leung CB, To KF, Lui SF, Szeto CC, Chung S, Sung JJ: A major outbreak of severe acute respiratory syndrome in Hong Kong. N Engl J Med 2003, 348:1986–1994
9. Peiris JS, Chu CM, Cheng VC, Chan KS, Hung IF, Poon LL, Law KI, Tang BS, Hon TY, Chan CS, Chan KH, Ng JS, Zheng BJ, Ng WL, Lai RW, Guan Y, Yuen KY, HKU/UCH SARS Study Group: Clinical progression and viral load in a community outbreak of coronavirus-associated SARS pneumonia: a prospective study. Lancet 2003, 361:1767–1772
10. Tsui PT, Kwok ML, Yuen H, Lai ST: Severe acute respiratory syndrome: clinical outcome and prognostic correlates. Emerg Infect Dis 2003, 9:1064–1069
11. Li W, Moore MJ, Vasilieva N, Sui J, Wong SK, Berne MA, Somasundaran M, Sullivan JL, Luzuriaga K, Greenough TC, Choe H, Farzan M: Angiotensin-converting enzyme 2 is a functional receptor for the SARS coronavirus. Nature 2003, 426:450–454
12. Li W, Zhang C, Sui J, Kuhn JH, Moore MJ, Luo S, Wong SK, Huang IC, Xu K, Vasilieva N, Murakami A, He Y, Marasco WA, Guan Y, Choe H, Farzan M: Receptor and viral determinants of SARS-coronavirus adaptation to human ACE2. EMBO J 2005, 24:1634–1643
13. Li F, Li W, Farzan M, Harrison SC: Structure of SARS coronavirus spike receptor-binding domain complexed with receptor. Science 2005, 309:1864–1868
14. Li W, Greenough TC, Moore MJ, Vasilieva N, Somasundaran M, Sullivan JL, Farzan M, Choe H: Efficient replication of severe acute respiratory syndrome coronavirus in mouse cells is limited by murine angiotensin-converting enzyme 2. J Virol 2004, 78:11429–11433
15. Imai Y, Kuba K, Rao S, Huan Y, Guo F, Guan B, Yang P, Sarao R, Wada T, Leong-Poi H, Crackower MA, Fukamizu A, Hui CC, Hein L, Uhlig S, Slutsky AS, Jiang C, Penninger JM: Angiotensin-converting enzyme 2 protects from severe acute lung failure. Nature 2005, 436:112–116
16. Kuba K, Imai Y, Rao S, Gao H, Guo F, Guan B, Huan Y, Yang P, Zhang Y, Deng W, Bao L, Zhang B, Liu G, Wang Z, Chappell M, Liu Y, Zheng D, Leibbrandt A, Wada T, Slutsky AS, Liu D, Qin C, Jiang C, Penninger JM: A crucial role of angiotensin converting enzyme 2 (ACE2) in SARS coronavirus-induced lung injury. Nat Med 2005, 11:875–879
17. Gu J, Korteweg C: Pathology and pathogenesis of severe acute respiratory syndrome. Am J Pathol 2007, 170:1136–1147
18. Nicholls JM, Poon LL, Lee KC, Ng WF, Lai ST, Leung CY, Chu CM, Hui PK, Mak KL, Lim W, Yan KW, Chan KH, Tsang NC, Guan Y, Yuen KY, Peiris JS: Lung pathology of fatal severe acute respiratory syndrome. Lancet 2003, 361:1773–1778
19. Zhang Y, Li J, Zhan Y, Wu L, Yu X, Zhang W, Ye L, Xu S, Sun R, Wang Y, Lou J: Analysis of serum cytokines in patients with severe acute respiratory syndrome. Infect Immun 2004, 72:4410–4415
20. Okabayashi T, Kariwa H, Yokota S, Iki S, Indoh T, Yokosawa N, Takashima I, Tsutsumi H, Fujii N: Cytokine regulation in SARS coronavirus infection compared to other respiratory virus infections. J Med Virol 2006, 78:417–424
21. Gao W, Tamin A, Soloff A, D'Aiuto L, Nwanegbo E, Robbins PD, Bellini WJ, Barratt-Boyes S, Gambotto A: Effects of a SARS-associated coronavirus vaccine in monkeys. Lancet 2003, 362:1895–1896
22. McAuliffe J, Vogel L, Roberts A, Fahle G, Fischer S, Shieh W, Butler E, Zaki S, Claire MS, Murphy B, Subbarao K: Replication of SARS coronavirus administered into the respiratory tract of African Green, rhesus and cynomolgus monkeys. Virology 2004, 330:8–15
23. Qin C, Wang J, Wei Q, She M, Marasco WA, Jiang H, Tu X, Zhu H, Ren L, Gao H, Guo L, Huang L, Yang R, Cong Z, Guo L, Wang Y, Liu Y, Sun Y, Duan S, Qu J, Chen L, Tong W, Ruan L, Liu P, Zhang H, Zhang J, Zhang H, Liu D, Liu Q, Hong T, He W: An animal model of SARS produced by infection of Macaca mulatta with SARS coronavirus. J Pathol 2005, 206:251–259

24. Rowe T, Gao G, Hogan RJ, Crystal RG, Voss TG, Grant RL, Bell P, Kobinger GP, Wivel NA, Wilson JM: Macaque model for severe acute respiratory syndrome. J Virol 2004, 78:11401–11404
25. Liang L, He C, Lei M, Li S, Hao Y, Zhu H, Duan Q: Pathology of guinea pigs experimentally infected with a novel reovirus and coronavirus isolated from SARS patients. DNA Cell Biol 2005, 24:485–490
26. Weingartl HM, Copps J, Drebot MA, Marszal P, Smith G, Gren J, Andova M, Pasick J, Kitching P, Czub M: Susceptibility of pigs and chickens to SARS coronavirus. Emerg Infect Dis 2004, 10:179–184
27. Roberts A, Vogel L, Guarner J, Hayes N, Murphy B, Zaki S, Subbarao K: Severe acute respiratory syndrome coronavirus infection of golden Syrian hamsters. J Virol 2005, 79:503–511
28. Martina BE, Haagmans BL, Kuiken T, Fouchier RA, Rimmelzwaan GF, Van Amerongen G, Peiris JS, Lim W, Osterhaus AD: SARS virus infection of cats and ferrets. Nature 2003, 425:915
29. Roberts A, Paddock C, Vogel L, Butler E, Zaki S, Subbarao K: Aged BALB/c mice as a model for increased severity of severe acute respiratory syndrome in elderly humans. J Virol 2005, 79:5833–5838
30. Sandmand M, Bruunsgaard H, Kemp K, Andersen-Ranberg K, Pedersen AN, Skinhoj P, Pedersen BK: Is ageing associated with a shift in the balance between type 1 and type 2 cytokines in humans? Clin Exp Immunol 2002, 127:107–114
31. Looney RJ, Falsey AR, Walsh E, Campbell D: Effect of aging on cytokine production in response to respiratory syncytial virus infection. J Infect Dis 2002, 185:682–685
32. Antonini JM, Roberts JR, Clarke RW, Yang HM, Barger MW, Ma JY, Weissman DN: Effect of age on respiratory defense mechanisms: pulmonary bacterial clearance in Fischer 344 rats after intratracheal instillation of Listeria monocytogenes. Chest 2001, 120:240–249
33. Boukhvalova MS, Yim KC, Kuhn KH, Hemming JP, Prince GA, Porter DD, Blanco JC: Age-related differences in pulmonary cytokine response to respiratory syncytial virus infection: modulation by anti-inflammatory and antiviral treatment. J Infect Dis 2007, 195:511–518
34. Nagata N, Iwata N, Hasegawa H, Fukushi S, Yokoyama M, Harashima A, Sato Y, Saijo M, Morikawa S, Sata T: Participation of both host and virus factors in induction of severe acute respiratory syndrome (SARS) in F344 rats infected with SARS coronavirus. J Virol 2007, 81:1848–1857
35. Inoue G: Effect of interleukin-10 (IL-10) on experimental LPS-induced acute lung injury. J Infect Chemother 2000, 6:51–60
36. Fukushi S, Mizutani T, Saijo M, Matsuyama S, Miyajima N, Taguchi F, Itamura S, Kurane I, Morikawa S: Vesicular stomatitis virus pseudotyped with severe acute respiratory syndrome coronavirus spike protein. J Gen Virol 2005, 86:2269–2274
37. Liem NT, Nakajima N, Phat LLP, Sato Y, Thach HN, Hung PV, San LT, Katano H, Kumasaka T, Oka T, Kawachii S, Matsushita T, Sata T, Kudo K, Suzuki K: H5N1-infected cells in lung with diffuse alveolar damage in exudative phase from a fatal case in Vietnam. Jpn J Infect Dis 2008, 61:157–160
38. Ohnishi K, Sakaguchi M, Kaji T, Akagawa K, Taniyama T, Kasai M, Tsunetsugu-Yokota Y, Oshima M, Yamamoto K, Takasuka N, Hashimoto S, Ato M, Fujii H, Takahashi Y, Morikawa S, Ishii K, Sata T, Takagi H, Itamura S, Odagiri T, Miyamura T, Kurane I, Tashiro M, Kurata T, Yoshikura H, Takemori T: Immunological detection of severe acute respiratory syndrome coronavirus by monoclonal antibodies. Jpn J Infect Dis 2005, 58:88–94
39. Cameron MJ, Bermejo-Martin JF, Danesh A, Muller MP, Kelvin DJ: Human immunopathogenesis of severe acute respiratory syndrome (SARS). Virus Res 2008, 133:13–19
40. Cameron MJ, Ran L, Xu L, Danesh A, Bermejo-Martin JF, Cameron CM, Muller MP, Gold WL, Richardson SE, Poutanen SM, Willey BM, Devries ME, Fang Y, Seneviratne C, Bosinger SE, Persad D, Wilkinson P, Greller LD, Somogyi R, Humar A, Keshavjee S, Louie M, Loeb MB, Brunton J, McGeer AJ, Kelvin DJ: Interferon-mediated immunopathological events are associated with atypical innate and adaptive immune responses in severe acute respiratory syndrome (SARS) patients. J Virol 2007, 81:8692–8706
41. Theron M, Huang KJ, Chen YW, Liu CC, Lei HY: A probable role for IFN-gamma in the development of a lung immunopathology in SARS. Cytokine 2005, 32:30–38
42. Huang KJ, Su IJ, Theron M, Wu YC, Lai SK, Liu CC, Lei HY: An interferon-gamma-related cytokine storm in SARS patients. J Med Virol 2005, 75:185–194
43. Schultz RM, Kleinschmidt WJ: Functional identity between murine gamma interferon and macrophage activating factor. Nature 1983, 305:239–240
44. Noble A, Macary PA, Kemeny DM: IFN-gamma and IL-4 regulate the growth and differentiation of CD8+ T cells into subpopulations with distinct cytokine profiles. J Immunol 1995, 155:2928–2937
45. Natanson C, Eichenholz PW, Danner RL, Eichacker PQ, Hoffman WD, Kuo GC, Banks SM, MacVittie TJ, Parrillo JE: Endotoxin and tumor necrosis factor challenges in dogs simulate the cardiovascular profile of human septic shock. J Exp Med 1989, 169:823–832
46. Meldrum DR: Tumor necrosis factor in the heart. Am J Physiol 1998, 274:577–595
47. Ware LB, Matthay MA: The acute respiratory distress syndrome. N Engl J Med 2000, 342:1334–1349
48. Roberts A, Deming D, Paddock CD, Cheng A, Yount B, Vogel L, Herman BD, Sheahan T, Heise M, Genrich GL, Zaki SR, Baric R, Subbarao K: A mouse-adapted SARS-coronavirus causes disease and mortality in BALB/c mice. PLOS Pathogens 2007, 3:23–37

Available online at www.sciencedirect.com
ScienceDirect
Virology 370 (2008) 173–183
VIROLOGY
www.elsevier.com/locate/yviro

Pharmacological cdk inhibitor *R*-Roscovitine suppresses JC virus proliferation

Yasuko Orba [a,b,c], Yuji Sunden [d,e], Tadaki Suzuki [a,c], Kazuo Nagashima [b,f], Takashi Kimura [a], Shinya Tanaka [b], Hirofumi Sawa [a,e,*]

[a] *Department of Molecular Pathobiology, Hokkaido University Research Center for Zoonosis Control, N18, W9, Kita-ku, 060-0818, Sapporo, Japan*
[b] *Laboratory of Molecular and Cellular Pathology, Hokkaido University Graduate School of Medicine, N15, W7, Kita-ku, 060-8638, Sapporo, Japan*
[c] *Research Fellow of the Japan Society for the Promotion of Science, Japan*
[d] *Laboratory of Comparative Pathology, Hokkaido University Graduate School of Veterinary Medicine, N18, W9, Kita-ku, 060-0818, Sapporo, Japan*
[e] *21st Century COE Program for Zoonosis Control, Hokkaido University, N18, W9, Kita-ku, 060-0818, Sapporo, Japan*
[f] *Department of Pathology, Sapporo Higashi-Tokushukai Hospital, N33, E13, Higashi-Ku, 065-0033, Sapporo, Japan*

Received 9 July 2007; returned to author for revision 22 August 2007; accepted 30 August 2007
Available online 4 October 2007

Abstract

The human *Polyomavirus* JC virus (JCV) utilizes cellular proteins for viral replication and transcription in the host cell nucleus. These cellular proteins represent potential targets for antiviral drugs against the JCV. In this study, we examined the antiviral effects of the pharmacological cyclin-dependent kinase (cdk) inhibitor *R*-Roscovitine, which has been shown to have antiviral activity against other viruses. We found that Roscovitine significantly inhibited the viral production and cytopathic effects of the JCV in a JCV-infected cell line. Roscovitine attenuated the transcriptional activity of JCV late genes, but not early genes, and also prevented viral replication *via* inhibiting phosphorylation of the viral early protein, large T antigen. These data suggest that the JCV requires cdks to transcribe late genes and to replicate its own DNA. That Roscovitine exhibited antiviral activity in JCV-infected cells suggests that Roscovitine might have therapeutic utility in the treatment of progressive multifocal leukoencephalopathy (PML).

Keywords: JC virus; Progressive multifocal leukoencephalopathy; Antiviral drug; Cyclin-dependent kinase; Roscovitine

Introduction

Progressive multifocal leukoencephalopathy (PML) is a fatal demyelinating disease of the central nervous system (CNS) that is caused by the human *Polyomavirus* JC virus (JCV). PML is characterized by a selective destruction of oligodendrocytes that leads to multiple areas of demyelination and the attendant loss of motor and sensory function and cognitive impairment. PML is often observed in individuals with compromised immune systems, such as those with acquired immunodeficiency syndrome (AIDS), advanced stage malignant tumors, or recent organ transplantation with immunosuppressive therapy. The incidence of PML is increasing due to the AIDS pandemic. To date, there is no effective and specific therapy for PML. The only therapeutic option for patients with PML is highly active antiretroviral therapy (HAART), which has been shown to improve the prognosis for AIDS-related PML patients (Albrecht et al., 1998). However, a substantial number of PML patients are unresponsive to antiretrovirals and some patients develop an immune reconstitution inflammatory syndrome as a result of antiretroviral treatment (Collazos et al., 1999). In fact, a multicenter study of HIV-positive patients with PML failed to show a significant benefit of cytarabine or cidofovir in addition to antiretroviral treatment (Hall et al., 1998; Marra et al., 2002). Since the 5-hydroxytryptamine-2A serotonin receptor has been recently identified as a cellular receptor for JCV (Elphick et al., 2004), serotonin antagonists are under consideration as therapeutic drugs for preventing the spread of JCV in the CNS. In addition, small interfering RNA-based therapeutics against JCV may be useful if the siRNA delivery system into the CNS is developed (Orba et al., 2004; Radhakrishnan et al., 2004).

* Corresponding author. Department of Molecular Pathobiology, Hokkaido University Research Center for Zoonosis Control, N18, W9, Kita-ku, 060-0818, Sapporo, Japan. Fax: +81 11 706 5185.
E-mail address: h-sawa@czc.hokudai.ac.jp (H. Sawa).

0042-6822/$ - see front matter © 2007 Elsevier Inc. All rights reserved.
doi:10.1016/j.virol.2007.08.034

The JCV is a small double-stranded DNA virus that encodes early proteins (large T antigen, small t antigen, and T′ antigen) and late proteins (VP1, VP2, VP3, and agnoprotein) but does not encode its own kinases. Replication of the JCV needs the cellular replication proteins of host cells, and specific cellular factors in JCV-permissive cells are likely to play a role in the replication of the JCV. The JCV shares 69% sequence homology at the nucleotide level with simian virus 40 (SV40), and JCV and SV40 belong to the *Polyomavirus* family. Both viruses produce large T antigen (TAg), which is necessary for the replication of viral DNA. It has been reported that phosphorylation of a single residue at threonine 124 (T124) by a kinase such as the cdc2 kinase (also known as cdk1) of SV40 TAg is important for the viral DNA replication (McVey et al., 1989,

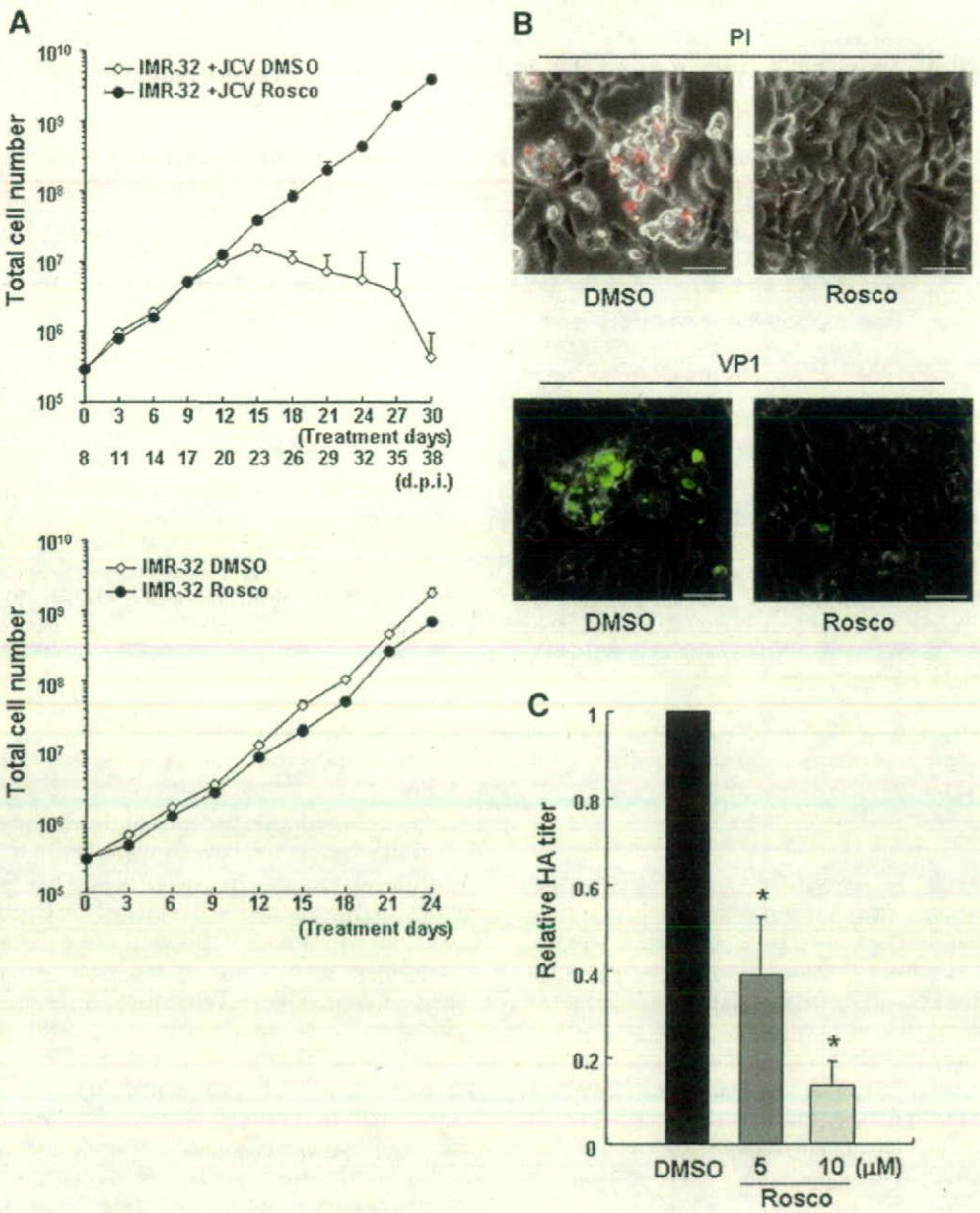

Fig. 1. Effects of Rosco on CPE of JCV-infected cells and JCV propagation. (A) Cell growth of IMR-32 cells or JCV-inoculated IMR-32 cells treated with DMSO (control) or Rosco (10 μM, dissolved in DMSO). Cells were treated every 3 days from 8 days post infection (d.p.i.) and the number of cells was counted at the indicated time points. (B) Induction of morphologic changes in JCV-inoculated IMR-32 cells treated with DMSO or Rosco at 23 d.p.i. Dead cells were examined with propidium iodide (PI) staining (red color). JCV-infected cells were stained with anti-VP1 antibody and Alexa 488-labeled secondary antibody (green color). Scale bars, 50 μm. (C) Hemagglutination activity (HA) of the JCV in JCI cells treated with DMSO or Rosco (5 or 10 μM) for 12 days. The HA titers of cell extracts from 1×10^6 cells are indicated as the normalized value for the cells treated with DMSO. These data represent the mean ± SD of the results from at least three independent experiments. *$p < 0.01$ versus the value for the cells treated with DMSO.

1993). Mutational analysis of the T124 residue of SV40 TAg has been shown to result in a replication defect in the initial steps of the sequence-specific unwinding of the core origin (Kim et al., 2002; McVey et al., 1996; Moarefi et al., 1993). Likewise, the cdk recognition sequence is conserved in the JCV TAg at threonine 125 (T125) (Swenson and Frisque, 1995). Mutation of the T125 residue of JCV TAg abolishes replication of JCV DNA (Swenson et al., 1996), suggesting that phosphorylation of the cdk recognition site of TAg is important for proper TAg function in viral DNA replication.

Cyclin-dependent kinases (cdks) are a family of serine/threonine kinases involved in the regulation of the cell cycle (cdk1, 2, 3, 4, 6, and 7), transcription (cdk7, 8, and 9), and neuronal functions (cdk5). The cdks associate with cyclin subunits and regulate the cell cycle by phosphorylating distinct cellular proteins, including transcription factors, histones, cytoskeletal proteins, and tumor suppressor proteins. The activity of cdks is positively regulated by cdk binding to a cyclin subunit and by phosphorylation on the kinase subunit in well-defined sites. Conversely, cdks are negatively regulated by phosphorylation at

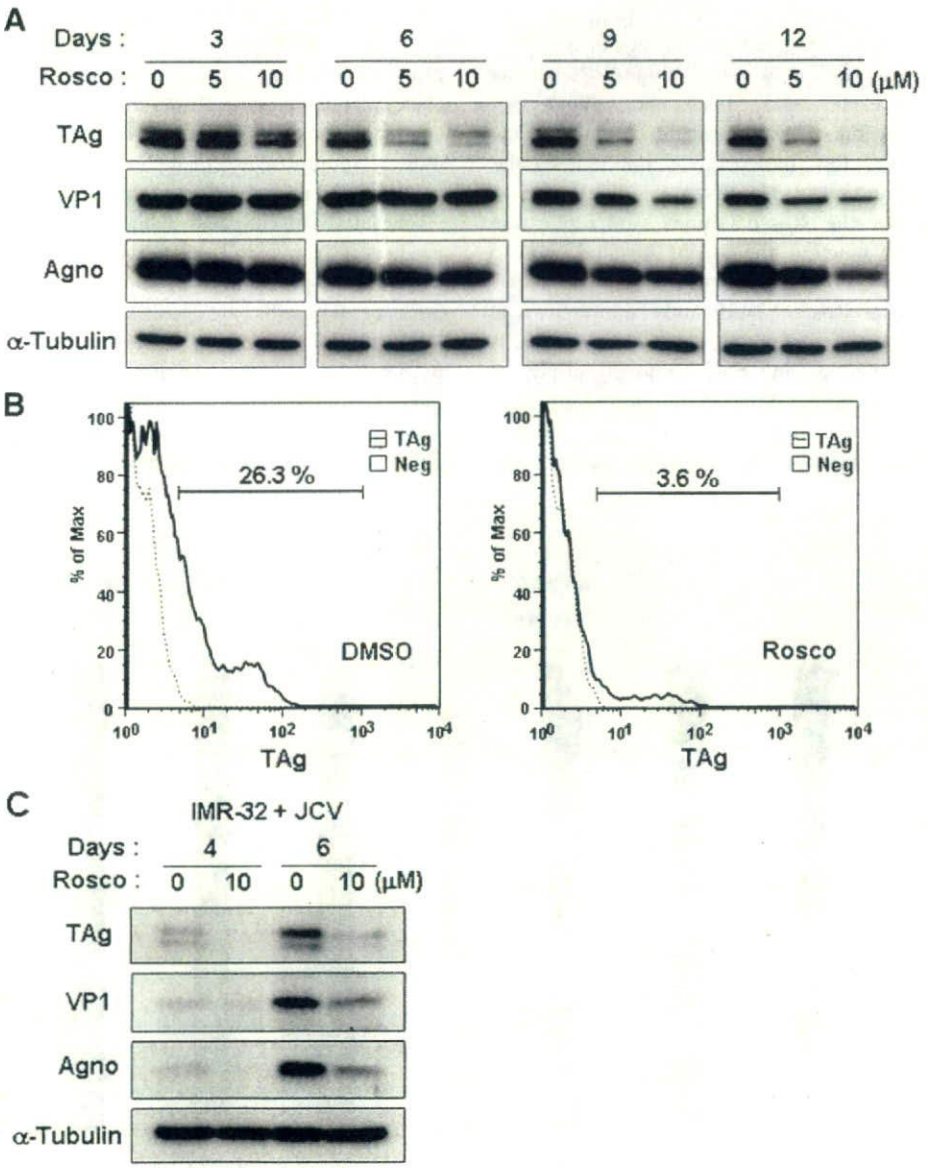

Fig. 2. Effects of Rosco on the expression of viral proteins. (A) Immunoblot analysis of viral proteins in JCI cells. Lysates prepared from JCI cells collected at 3, 6, 9, and 12 days after DMSO or Rosco (5 or 10 μM) treatment were used for immunoblotting with anti-TAg, -VP1, -Agno, and -alpha-tubulin antibodies. (B) Flow cytometry analysis of JCI cells treated with DMSO or Rosco (10 μM) for 10 days. TAg expressing cells were stained with anti-TAg antibody and FITC-labeled secondary antibody (black line) or secondary antibody only (gray dotted line). The percentage of TAg-positive cells is indicated on the panels. (C) Immunoblot analysis of viral proteins in JCV-inoculated IMR-32 cells. IMR-32 cells were inoculated with the JCV and treated with DMSO or Rosco (10 μM) for 4 or 6 days. Immunoblotting was performed using the same antibodies as in panel A.

different sites or by binding a natural cdk inhibitor, such as a member of the Cip/Kip or INK4 family.

Because cdks are required for the replication of many clinically important viruses, pharmacological cdk inhibitors (PCIs) have been proposed as potential antiviral drugs in recent years (Schang, 2002, 2004). *R*-Roscovitine (Rosco) is one of the purine-type PCIs that specifically inhibits cdk1, 2, 5, 7, and 9 by competing with ATP binding in the ATP binding pocket of the cdks (Canduri et al., 2004; De Azevedo et al., 1997; McClue et al., 2002; Meijer et al., 1997). Rosco has been proven non-toxic in animal models and is currently in phase II clinical trials to treat cancer and glomerulonephritis (Benson et al., 2007; McClue et al., 2002; Raynaud et al., 2005). Additionally, the study for tissue distribution and pharmacokinetics of Rosco in rat shows that brain exposure to Rosco is about 30% of that found in plasma (Vita et al., 2005). These data indicate that Rosco crosses the blood brain barrier probably because of the lipophilic character and low molecular weight (molecular weight=354) of the drug (Vita et al., 2005).

Since we hypothesize that Rosco inhibits viral replication *via* decreased JCV TAg function, the aim of this study was to examine the effects of Rosco on JCV proliferation. The results of this study show that Rosco significantly inhibited viral production and expression of viral proteins in JCV-infected cells by preventing viral replication and transcriptional activity of JCV late genes. We also confirmed that Rosco decreased phosphorylation of the cdk recognition motif on TAg. Thus, Rosco exhibits antiviral activity against JCV infection *in vitro*.

Results

Rosco inhibits JCV-induced CPE and JCV production

To test whether Rosco affected JCV propagation in host cells, we initially observed cell growth and the cytopathic effects (CPE) of the JCV (Wroblewska et al., 1980) using the JCV-permissive cell line, IMR-32. IMR-32 cells were inoculated with the JCV and at 8 days post-infection (d.p.i.), either DMSO or 10 μM Rosco (dissolved in DMSO) were added to the cells every 3 days for 30 days. At 23 d.p.i., CPE characterized by cell shrinkage and aggregation was observed in the control cells that were treated with DMSO alone (Figs. 1A and B). These aggregated cells were stained with propidium iodide, and JCV late protein, VP1 was also recognized in the cells (Fig. 1B). However, cells treated with Rosco did not show CPE and cell death even after inoculation with the JCV (Figs. 1A and B). Furthermore, 1-month treatment with Rosco (10 μM) did not induce apparent cell growth arrest of the IMR-32 cells (Fig. 1A).

We next investigated whether Rosco could affect JCV production using JCI cells, which come from an IMR-32-derived JCV-producing cell line in which approximately 10 to 20% of the cells are positive for JCV encoding protein (Nukuzuma et al., 1995). To test the effect of Rosco on JCV production in JCI cells, we measured viral HA titers of the cells treated with DMSO or Rosco (5 or 10 μM) for 12 days. The HA titer was significantly and dose-dependently decreased in cells treated with Rosco compared to cells treated with DMSO

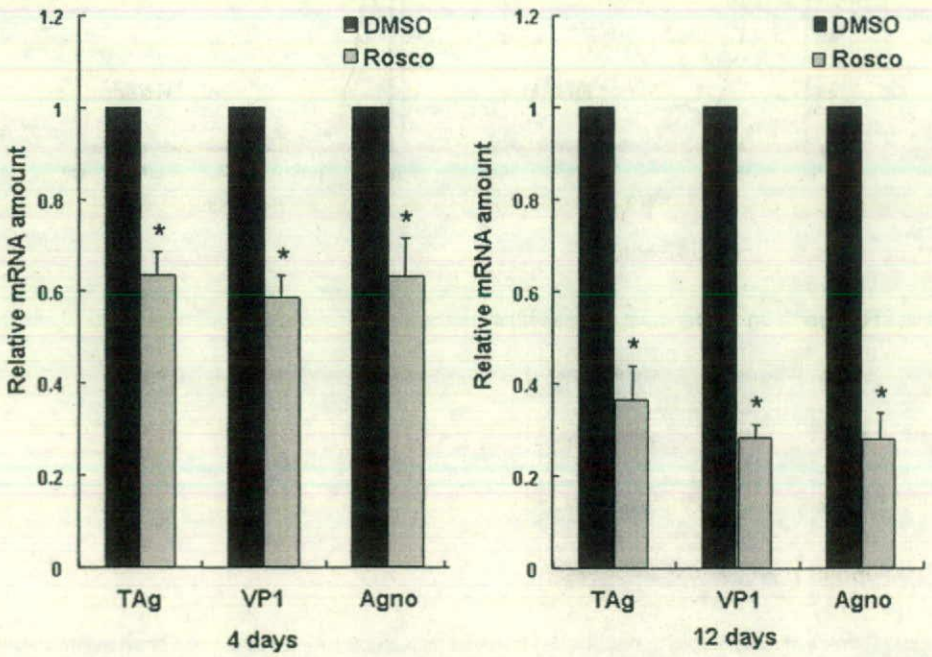

Fig. 3. Effects of Rosco on viral mRNA production in JCI cells. JCI cells were treated with DMSO or Rosco (10 μM) for 4 or 12 days and total RNA was isolated from the cells. Viral mRNAs were measured by quantitative RT-PCR using specific primer sets for JCV TAg, VP1, and Agno. The data are normalized to the amount of beta actin mRNA and are expressed as the ratio of mRNA levels in Rosco-treated cells to DMSO-treated cells. These data represent the mean ± SD of the results from at least three independent experiments. *$p<0.01$ versus the value for the cells treated with DMSO.

(Fig. 1C). These data indicated that Rosco suppresses JCV production and cell death caused by JCV infection without affecting host cell growth.

Rosco inhibits the expression of JCV proteins

Next we examined the expression of viral proteins when JCI cells were treated with DMSO or Rosco (5 or 10 μM) every 3 days for 12 days. Rosco dose-dependently decreased expression of TAg at 3 days and decreased expression of VP1 and agnoprotein (Agno) at 9 days (Fig. 2A). We also examined the number of JCV-infected cells in JCI cells treated with Rosco. Flow cytometry analysis indicated that TAg-expressing cells were substantially decreased after treatment with 10 μM Rosco for 10 days (Fig. 2B). We did not observe a decrease in early and late protein expression until 3 and 9 days, respectively, because the JCV genome had already proliferated in JCI cells and the stage of JCV infection in each cell was diverse in JCI cells. Therefore, we examined the effect of Rosco on the expression of viral proteins in JCV-inoculated IMR-32 cells. IMR-32 cells were inoculated with the JCV and simultaneously treated with DMSO or Rosco (10 μM) for 4 or 6 days. As expected, Rosco markedly suppressed the expression of both early and late proteins, whereas viral proteins were detected at 4 days after JCV inoculation in the cells treated with DMSO (Fig. 2C).

To confirm whether the reduction of viral protein expression by Rosco was caused by the inhibition of viral protein production, we measured the amount of viral mRNA in JCI cells treated with Rosco (10 μM) for 4 or 12 days. Using quantitative RT-PCR, we found that the amount of early and late mRNA was significantly decreased at 4 and 12 days after treatment with Rosco (Fig. 3). Thus, Rosco potently decreased overall viral burden in JCV-infected cells.

Rosco inhibits the transcriptional activity of JCV late genes

Although expressions of both early and late mRNAs were decreased in JCI cells treated with Rosco (Fig. 3), these results

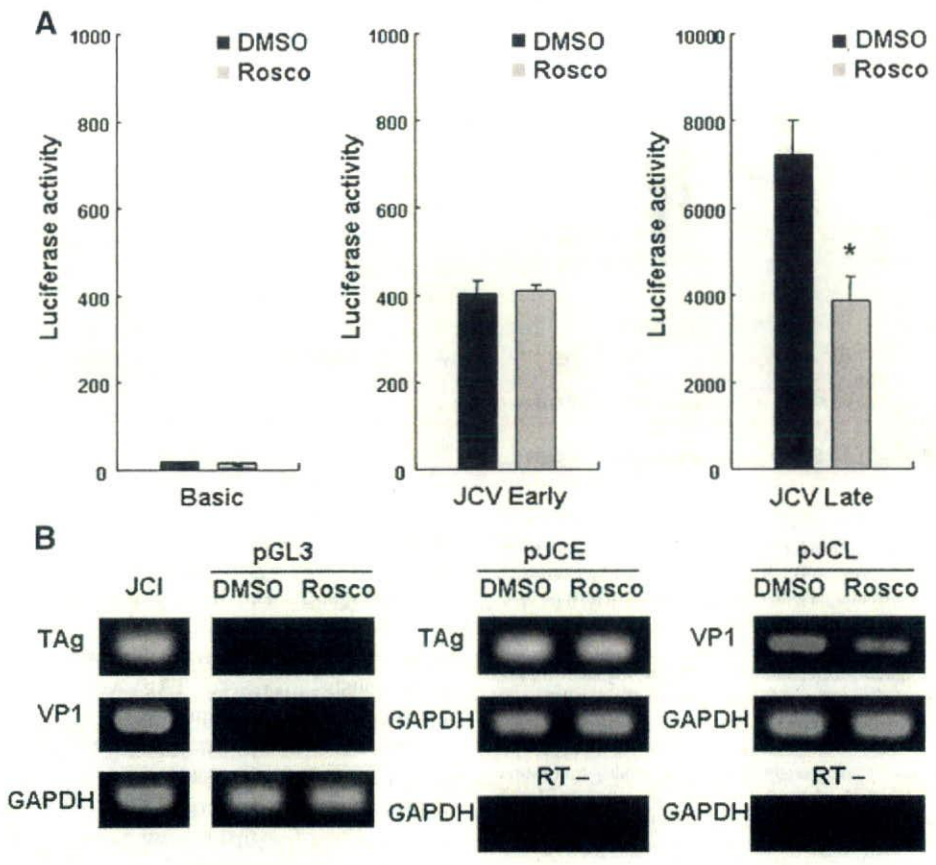

Fig. 4. Effects of Rosco on JCV early and late promoter activity. (A) Luciferase assay for the JCV promoter. After pretreatment with DMSO or Rosco (10 μM) for 48 h, IMR-32 cells were transfected with luciferase reporter plasmids containing the JCV early promoter (pGL3-early), late promoter (pGL3-Late), or empty vector (pGL3-Basic). Cells were cultured with DMSO or Rosco for 48 h and the luciferase activity of the cell extracts was measured. These data represent the mean ± SD of the results from at least three independent experiments. *$p < 0.01$ versus the value for the cells treated with DMSO. (B) Transcription assay for the JCV early and late genes. IMR-32 cells were transfected with an empty vector (pGL3), JCV early genes (pJCE), or late genes (pJCL) and treated with DMSO or Rosco for 48 h. RT-PCR was performed on the total RNA extracted from the cells. To detect pJCE- or pJCL-specific transcripts, PCR analysis of the synthesized cDNA was carried out using primers for TAg or VP1, respectively. GAPDH was used as an internal control. RNA from JCI cells were used as positive control.

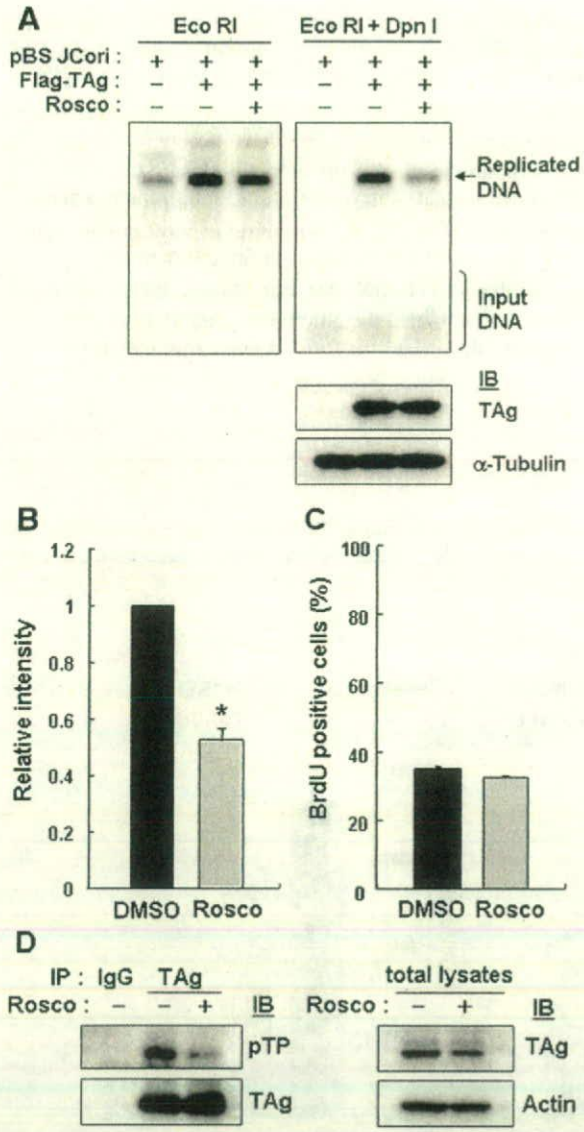

Fig. 5. Effects of Rosco on JCV replication activity. (A) Representative Southern blot from the replication assay. IMR-32 cells were transfected with plasmids containing the JCV replication origin (pBS-JCori) and either a TAg expression vector or mock vector and were cultured with DMSO or Rosco (10 μM) for 48 h. Low molecular weight DNA was isolated from cells and digested with *Eco*RI or *Eco*RI and *Dpn*I. Southern blots were performed by hybridization of a digoxigenin-labeled probe against an ampicillin-resistant gene fragment of pBS-JCori. Immunoblot (IB) analysis of Flag-TAg expression in these cells is also indicated. (B) The signals for replicated DNA were quantified with an image analyzer and plotted as a value that is normalized to the cells treated with DMSO. These data represent the mean±SD of the results from three independent experiments. $*p<0.01$ versus the value for the cells treated with DMSO. (C) Cellular genomic replication was measured by BrdU incorporation. BrdU was incorporated into IMR-32 cells for 1 h after treatment with DMSO or Rosco (10 μM) for 48 h. The percentage of BrdU-positive cells was measured by flow cytometry analysis. (D) Effects of Rosco on TAg phosphorylation by cdk. Lysates prepared from JCI cells collected at 48 h after DMSO or Rosco (10 μM) treatment were used for immunoprecipitation (IP) with an anti-TAg antibody or normal mouse IgG. Immunoblotting (IB) was performed with an anti-TAg antibody and anti-phospho-threonine proline (pTP) antibody that recognizes cdk phosphorylation sites. Immunoblots were also performed on total lysates using anti-TAg and actin antibodies.

indicate overall burden of viral infection in JCI cells as measured in the presence of early and late proteins and viral DNA and not represent transcriptional activity of the JCV promoter itself. Therefore, to investigate whether Rosco-induced suppression of viral mRNA production is related to the viral transcriptional activity, we examined activity of the JCV promoter in IMR-32 cells in the presence or absence of Rosco. Because the transcriptional control region (TCR) of the JCV is comprised of the bidirectional promoter that drives viral early and late transcripts in opposite directions, we performed a luciferase assay using luciferase reporter plasmids containing the JCV early or late promoter in IMR-32 cells. When cells were treated with Rosco (10 μM) for 48 h after transfection with reporter plasmids, the transcriptional activity of the JCV late promoter was significantly decreased compared to that of control cells, whereas the activity of the early promoter was unchanged by Rosco (Fig. 4A). Furthermore, these results were confirmed using plasmids designated pJCE or pJCL that contained the JCV TCR and the downstream early or late JCV genome, respectively. Consistent with the results of the luciferase assay, expression of the VP1 transcript was inhibited by Rosco treatment (Fig. 4B). Thus, Rosco inhibited transcriptional activity of the JCV late genes, but not early genes.

Rosco inhibits JCV replication

JCV TAg has the cdk recognition motif at threonine 125 (T125), and it has been suggested that phosphorylation of this site by cdk plays a key role in the replication activity of TAg. Therefore, we examined the effects of Rosco on JCV replication using a *Dpn*I replication assay in IMR-32 cells. Because JCV replication is dependent on TAg, IMR-32 cells were co-transfected with a TAg expression vector and pBS-JCori, which contains the JCV TCR including the replication origin. After treatment with DMSO or Rosco (10 μM) for 48 h, viral DNA replication was assessed by Southern blot analysis of *Eco*RI and *Dpn*I-digested low molecular weight DNA extracted from the cells. We detected *Dpn*I-resistant replication products in the presence of TAg, whereas replication was significantly decreased after treatment with Rosco (Figs. 5A and B). We also used a BrdU incorporation assay to show that Rosco did not affect the replication of cellular DNA (Fig. 5C). In this experiment, the amounts of exogenously expressed TAg were not different between DMSO and Rosco-treated cells (Fig. 5A); therefore, the inhibition of viral DNA replication by Rosco is not likely to result from TAg depletion, but rather a result of post-translational modification of TAg, for example, by phosphorylation. Thus, TAg that was immunoprecipitated from JCI cells was probed with an antibody that recognizes cdk threonine phosphorylation sites to examine if Rosco affected the phosphorylation of the cdk recognition motif on TAg. As we expected, phosphorylation of the cdk recognition motif on TAg was markedly decreased in the cells treated with Rosco (Fig. 5D). These data indicate that Rosco inhibited JCV replication by preventing the phosphorylation of TAg.

Discussion

Several recent studies have suggested that the effects of Rosco *in vitro* might have antiviral therapeutic utility against human cytomegalovirus (HCMV), herpes simplex virus (HSV) type 1 and 2, human immunodeficiency virus type-1 (HIV-1), Epstein-Barr virus (EBV), varicella-zoster virus (VZV), and some other viruses (Bresnahan et al., 1997; Kudoh et al., 2004; Schang et al., 1998; Taylor et al., 2004; Wang et al., 2001). Rosco has been shown to inhibit not only viral DNA replication, but also transcription, post-translational modification, and subcellular localization of viral proteins (Davido et al., 2002; Habran et al., 2005; Sanchez et al., 2004; Sanchez and Spector, 2006). Moreover, Rosco exerts these effects against mutant strains of these viruses that are resistant to conventional antiviral drugs because it targets cellular cdks instead of viral proteins (Agbottah et al., 2005; Schang et al., 2002).

In this study, we demonstrated that Rosco exhibits antiviral effects against the JCV. Rosco effectively suppressed viral propagation and the expression of viral proteins in JCI cells and JCV-inoculated IMR-32 cells at 10 μM. Transcription and replication assays for the JCV indicated that the antiviral effects of Rosco on the JCV were responsible for the suppression of both the transcriptional activity of the JCV late promoter and the replication of viral DNA. In addition to TAg, many cellular transcription factors such as NF1, NF-κB, Tst-1, YB-1, and AP1 are known to be involved in controlling JCV late transcription (Amemiya et al., 1989; Kerr et al., 1994; Ranganathan and Khalili, 1993; Sadowska et al., 2003; Wegner et al., 1993). Since Rosco inhibited the transcription of late proteins in the absence of TAg, it seems likely that some cellular protein(s), including unknown molecule(s) which transactivate the JCV late promoter, are regulated by cdk. As for the effect of Rosco on viral replication, the inhibition of TAg phosphorylation at the cdk recognition motif by Rosco results in defective viral replication because functional phosphorylated TAg is essential for JCV replication. These data suggest that the JCV requires cdk for the transcription of late genes, as well as for replication of its own DNA. It is known that JCV-infected oligodendrocytes in the brains of individuals with PML overexpress Ki-67, cyclin A, and cyclin B1, which are normally regulated in a cell-cycle-specific manner (Ariza et al., 1998). The JCV is more likely to induce cellular cdk/cyclin activity for self-replication of its genome in mature oligodendrocytes, which are thought to exist in a non-proliferating state (Ruffini et al., 2004).

Many antiviral drugs have been designed to target viral proteins to avoid cytotoxicity. However, this approach seems to be difficult with small viruses like the JCV that encode a limited number of proteins. Alternatively, antiviral drugs that target cellular proteins might exhibit activity against many viruses, including small viruses, because the replication of many viruses requires cellular proteins. Antiviral drugs that target cellular proteins seem to be active even against mutated viruses that are resistant to conventional antiviral drugs. Furthermore, antiviral reagents that target common cellular proteins that are required by different viruses might be particularly effective treatments for infections of multiple viruses, for example, JCV and HIV in the case of AIDS-related PML. A potential drawback of targeting cellular proteins is the presumably greater risk of cytotoxicity or side-effects; therefore, the potential cytotoxic effects of antiviral drugs that target cellular proteins should be carefully examined *in vivo*. Thus far, no major toxic effects of Rosco have been reported in pre-clinical and clinical trials, even though PCIs target cellular cdks (Benson et al., 2007; McClue et al., 2002; Raynaud et al., 2005). Furthermore, pharmacokinetic data for Rosco indicates that it crosses the blood brain barrier in rat (Vita et al., 2005), which is important for the treatment of CNS diseases such as PML. Thus, Rosco shows substantial promise as a clinical antiviral drug that might be effective against PML.

Materials and methods

Cells and virus infection

Cells from the human neuroblastoma cell line IMR-32 (HSRRB, Osaka, Japan) and JCV-producing JCI cells that were derived from the IMR-32 cell line (Nukuzuma et al., 1995) were maintained at 37 °C and 5% CO_2 in Dulbecco's minimal essential medium (DMEM) supplemented with 10% fetal bovine serum (FBS), antibiotics, 2 mM L-glutamine, and 0.1 mM non-essential amino acids.

For virus preparation, JCI cells were harvested and suspended in Tris-HCl (pH 7.5) containing 0.2% bovine serum albumin (BSA), frozen and thawed three times, and then treated with 0.05 U/ml of neuraminidase type V (Sigma, St. Louis, MO) at 37 °C for 16 h. After incubation at 56 °C for 30 min, cell lysates were centrifuged at 1,000×*g* for 10 min. The supernatant was quantified by hemagglutination (HA) assays and stored at −80 °C until use. For virus infection, IMR-32 cells were inoculated with 200 HA/ml of the JCV in growth media for 24 h. Following inoculation, the cells were cultured in fresh media until assay.

Chemicals and antibodies

A 50 mM stock solution of Roscovitine (Calbiochem, Darmstadt, Germany) was prepared in dimethylsulfoxide (DMSO, Sigma).

The anti-VP1 antibody was generated by immunizing rabbits with virus-like particles prepared from recombinant VP1 expressed in *Escherichia coli* (Komagome et al., 2002). The anti-agnoprotein antibody was generated by immunizing rabbits with a synthetic peptide from the agnogene of the Mad1 strain of the JCV (Endo et al., 2003). The monoclonal anti-SV40 TAg (Ab-2) antibody, which has been previously shown to cross-react with the JCV large T (Okada et al., 2002), was obtained from Calbiochem. The monoclonal anti-actin (Chemicon, Temecula, CA), monoclonal anti-α-tubulin (Sigma), monoclonal anti-phospho-Threonine cdk substrate (Cell Signaling Technology, Beverly, MA), and Rat monoclonal anti-BrdU (Abcam, Cambridge, UK) antibodies were commercially obtained.

Drug treatment and viable cell count

Either DMSO or 10 μM Rosco was diluted in media and added to cells every 3 days for 30 days when the cells were passaged. At the same time, the number of cells was determined by counting the viable cells with a hemocytometer using the Trypan blue dye exclusion assay. For each period, three dishes of each group were counted. At 23 d.p.i., cells were stained with 2 μg/ml of propidium iodide (PI) in growth media, then CPE- and PI-positive cells were evaluated under an inverted fluorescence/phase-contrast microscopy (Olympus, Tokyo, Japan).

Hemagglutination (HA) assay

JCV titers were assayed by hemagglutination of human type O erythrocytes as described previously (Suzuki et al., 2001). JCI cells were collected after treatment with 0 μM (DMSO only), 5 μM, or 10 μM of Roscovitine for 12 days. The media, with or without Roscovitine, were changed every 3 days. The cells (1×10^6) were washed in phosphate-buffered saline (PBS), re-suspended with 50 μl of Tris-HCl (pH 7.5) containing 0.2% BSA, and treated with 0.05 U/ml of neuraminidase as described above. For the hemagglutination assay, two-fold serial dilutions of the cell extract (25 μl) with PBS (pH 7.15) containing 0.2% BSA were made in 96-well, V-bottomed microplates. An equal volume of 0.5% red blood cells in PBS (pH 7.15) was added to each well. Cells were incubated at 4 °C for 3 h, at which point the HA titer of virus was expressed as the highest dilution resulting in hemagglutination.

Immunocytochemistry

JCV-infected IMR-32 cells were fixed for 3 min in 100% methanol at −20 °C. After blocking with 1% BSA, cells were incubated with anti-VP1 antibody (1:5,000) overnight at 4 °C, and stained with Alexa Fluor 488-conjugated anti-rabbit immunoglobulin antibody (1:500; Invitrogen, Carlsbad, CA) for 1 h at room temperature. Cells positive for VP1 were observed under an inverted fluorescence/phase-contrast microscopy (Olympus).

Immunoblotting and immunoprecipitation

Either IMR-32 cells inoculated with 800 HA units of the JCV in 4 ml of growth media or JCI cells were collected at various days in the presence or absence of Rosco and lysed in lysis buffer [1% Triton X-100, 150 mM NaCl, 0.1% sodium dodecyl sulfate (SDS), 1% deoxycholic acid, 10 mM Tris-HCl (pH 7.5), 5 mM EDTA, 10% glycerol, 50 mM sodium fluoride, and 1 mM phenylmethylsulfonyl fluoride]. After sonication and centrifugation, 10 μg of protein was separated by SDS–PAGE and examined by immunoblotting using anti-VP1 (1:5,000), anti-agnoprotein (1:3,000), anti-SV40 large T (1:500), and anti-α-tubulin (1:5,000) antibodies. After incubation with horseradish peroxidase-conjugated secondary antibody (1:3,000; Biosource International, Camarillo, CA), the signal was detected with an ECL detection kit (GE Healthcare Bio-Sciences, Piscataway, NJ) and visualized with a LAS-1000 plus system (Fujifilm, Tokyo, Japan).

For immunoprecipitation, cells were lysed in IP lysis buffer [1% NP40, 150 mM NaCl, 10 mM Tris-HCl (pH 7.5), 1 mM EDTA, 50 mM sodium fluoride, 1 mM phenylmethylsulfonyl fluoride, 1 mM sodium orthovanadate, complete protease inhibitor cocktail (Roche, Basel, Switzerland), and phosphatase inhibitor cocktail 1 (Sigma)]. Lysed protein was pre-incubated with 20 μl of protein G Sepharose (GE Healthcare Bio-Sciences) at 4 °C for 1 h. The supernatant was incubated with anti-large T antibody or normal mouse IgG at 4 °C for 3 h. Protein complexes were pulled down by incubation with protein G Sepharose at 4 °C for 2 h and elution with SDS sample buffer [125 mM Tris-HCl (pH 6.8), 10% 2-mercaptoethanol, 4% SDS, 10% sucrose, and 0.04% bromophenol blue] after washing with IP lysis buffer. Immunoblotting was carried out with the anti-phospho-Thr-Pro antibody (1:5,000) and horseradish peroxidase-conjugated anti-mouse IgM (1:3,000; Zymed, South San Francisco, CA) secondary antibody. Signals were analyzed as described above.

Flow cytometry

For flow cytometry analysis of TAg expression, JCI cells were collected, washed twice with PBS, suspended, and fixed with 70% ice-cold ethanol overnight at 4 °C. Cells were washed with PBS containing 0.5% fetal bovine albumin, incubated with anti-SV40 TAg (Ab-2) antibody at room temperature for 2 h and stained with fluorescein isothiocyanate (FITC)-conjugated anti-mouse IgG (Beckman Coulter, Fullerton, CA) at room temperature for 1 h. Flow cytometry experiments were carried out using a FACSCalibur system (BD Biosciences, Sun Jose, CA) and data were analyzed using Flowjo software (Tree Star, Ashland, OR).

Reverse transcription (RT) and real-time PCR

For RNA extraction, JCI cells were collected after varying durations of treatment with DMSO or 10 μM Roscovitine. Total RNA was isolated using an RNeasy Mini Kit (Qiagen, Valencia, CA) according to the manufacturer's protocol. Total RNA (1 μg) was treated with DNase I (Invitrogen) at 37 °C for 1 h in 10 μl of reaction mixture. After inactivation of DNase I with 2.5 mM EDTA at 65 °C for 15 min, 4 μl of reaction mixture was used for RT using a Superscript first-strand synthesis system (Invitrogen). To confirm that the samples were not contaminated with genomic DNA, RNase-free water was added instead of Superscript II reverse transcriptase to at least one negative control sample that was run in parallel. After confirmation of cDNA amplification by conventional PCR for β-actin and VP1, real-time PCR was performed using 0.5 μl of reaction mixture containing cDNA, SYBR green PCR Master Mix (Applied Biosystems, Foster City, CA), and gene-specific primer sets: JCV large T, 5′-AAA GTT GCT CAT CAG CCT GAT TTT-3′ and 5′-CAT CCC ACT TCT CAT TAA ATG TAT TCC-3′; JCV agnoprotein, 5′-CCA GCT GTC ACG TAA GGC TTC T-3′ and 5′-GTG CAA AAG TCC AGC AAA AAT TC-3′; JCV VP1, 5′-

TCT AAA TGA GGA TCT AAC CTG TGG AAA-3′ and 5′-GCC CAT TAG AGT GCA CAT TCA TC-3′; β-actin, 5′-TTG CCG ACA GGA TGC AGA A-3′ and 5′-GCC GAT CCA CAC GGA GTA CT-3′. After incubation of mixtures at 50 °C for 2 min and 95 °C for 10 min, the reaction was performed at 95 °C for 15 s and 60 °C for 1 min for 40 cycles using a GeneAmp 5700 Sequence Detection System (Applied Biosystems). The levels of PCR products were analyzed with GeneAmp 5700 SDS software (Applied Biosystems) and cycle times were normalized to the cycle time of β-actin (Orba et al., 2004). All reactions were confirmed by at least three independent experiments.

Luciferase assay and JCV transcription assay

Firefly luciferase reporter vectors pGL3-Basic and the internal *Renilla* luciferase control vector phRL-TK were purchased from Promega (Madison, WI). JCV early and late reporter vectors (pGL3-Early or pGL3-Late) were constructed from the regulatory regions of JCV Mad1 that has been previously described (Okada et al., 2000). For the luciferase assay, IMR-32 cells were seeded onto 24-well plates and the cells were treated with DMSO or 10 μM Roscovitine for 48 h. Each pGL3 reporter vector and phRL-TK control vector were co-transfected into the cells using Lipofectamine 2000 (Invitrogen) according to the manufacturer's instructions. Six hours after transfection, the media on each plate of cells were replaced with fresh media containing DMSO or Roscovitine and the cells were cultured for another 48 h. Luciferase activity of the cells was measured using a dual-luciferase reporter assay system (Promega) according to the manufacturer's instructions. Luminescence intensity was measured with a Luminometer (Turner Designs, Sunnyvale, CA). The firefly luciferase activity data are presented as mean values±SD. The results of each experiment were confirmed by three independent transfections. We could not use *Renilla* luciferase activity for normalization of the firefly luciferase activity because Roscovitine seems to affect *Renilla* luciferase activity derived from phRL-TK with the HSV-TK promoter (Schang et al., 1999). The pJCE and pJCL reporter plasmids for the analysis of JCV transcriptional activity were constructed as follows: the early (E) and late (L) genes of the JCV Mad1 strain containing the TCR and poly-adenylation signal were amplified by PCR and subcloned into pGL3-basic that had been digested with *Nhe*I and *Sal*I. IMR-32 cells were seeded onto 6-well plates and transfected with pGL3 basic, pJCE, or pJCL. Six hours after transfection, the media on each plate of cells were replaced with fresh media containing DMSO or Roscovitine and the cells were cultured for 48 h. RNA extraction and reverse transcription were performed as described above. To detect pJCE- or pJCL-specific transcripts, PCR analyses of the synthesized cDNA were carried out using Taq DNA polymerase (Sigma). For detection of early transcripts, the primer pairs of JCV large T: 5′-AAA GTT GCT CAT CAG CCT GAT TTT-3′ and 5′-CAT CCC ACT TCT CAT TAA ATG TAT TCC-3′, and for late transcripts, the primer pairs of JCV VP1: 5′-AAT GTG CAC TCT AAT GGG CAA GC-3′ and 5′-CTA GGT ACG CCT TGT GCT CTG-3′ were used. As a control, the primer pairs of glyceraldehyde 3-phosphate dehydrogenase (GAPDH): 5′-TTC GTC ATG GGT GTG AAC CA-3′ and 5′-GGT CAT GAG TCC TTC CAC GAT AC-3′ were used.

DpnI replication assay

The full-length of the JCV Mad1 transcriptional control region (TCR) was subcloned into a pBluescript II SK (+) vector, which was designated pBS-JCori. The JCV TAg expression vector $pCXN_2$-JCTAg was constructed from pBR-Mad1. IMR-32 cells were seeded onto 6 cm dishes and co-transfected with pBS-JCori and $pCXN_2$-JCTAg or a $pCXN_2$ empty vector using Lipofectamine 2000 according to the manufacturer's instructions. Six hours after transfection, the media on each plate of cells were replaced with fresh media containing DMSO or 10 μM Roscovitine and cells were cultured for 48 h. Low-molecular weight DNA was isolated from the cells according to the method of Hirt (1967). Extracts were treated with 0.5 mg/ml Proteinase K at 56 °C for 1 h prior to phenol/chloroform/isoamyl alcohol and ethanol precipitation. DNA was suspended in TE [10 mM Tris-HCl (pH 7.5), 1 mM EDTA (pH 8.0)] containing 75 μg/ml RNase A. Sample DNA (5 μg) was digested with *Eco*RI and *Dpn*I, which selectively digest transfected DNA that has been methylated during prokaryotic replication, and digested products were separated by electrophoresis on a 1% agarose gel. DNA fragments were transferred to a Hybond N^+ membrane (GE Healthcare Bio-Sciences) by capillary transfer using 20× SSC transfer buffer. The immobilized DNA was detected using a digoxigenin-labeled DNA probe that encoded a vector-derived ampicillin-resistant DNA sequence (DIG high prime DNA labeling and detection starter kit II, Roche). Signals were visualized with the LAS-1000 plus system and replication activities were determined by quantifying the intensity of the bands using Multi Gauge software (Fujifilm). These results were confirmed by three independent experiments.

BrdU incorporation

For detection of BrdU incorporation by flow cytometry, 10 μM of BrdU (Sigma) was incorporated into the cells for 1 h after treatment with DMSO or 10 μM Roscovitine for 2 days. Cells were washed twice with PBS and suspended and fixed with 70% ice-cold ethanol overnight. DNA was denatured with 2 N HCl in PBS containing 0.1% Triton-X at room temperature for 20 min and neutralized with 0.1 M Sodium tetraborate (pH 9.0) for 5 min. Treated cells were washed in PBS containing 0.5% BSA, stained with Rat anti-BrdU antibody (1:50), and stained with FITC-conjugated anti-Rat IgG antibody. BrdU-positive cells were analyzed by flow cytometry as described above.

Statistics

Statistical comparisons between experimental groups were analyzed using the Student's *t*-test, and for all comparisons $p<0.05$ was considered significant.

Acknowledgments

This study was supported in part by grants from the Ministry of Education, Science, Sports, and Culture and by grants from the Ministry of Health, Labor and Welfare, Japan; the Japan Health Science Foundation; and the Program of Founding Research Centers for Emerging and Reemerging Infectious Diseases, MEXT Japan.

References

Agbottah, E., de La Fuente, C., Nekhai, S., Barnett, A., Gianella-Borradori, A., Pumfery, A., Kashanchi, F., 2005. Antiviral activity of CYC202 in HIV-1-infected cells. J. Biol. Chem. 280 (4), 3029–3042.

Albrecht, H., Hoffmann, C., Degen, O., Stoehr, A., Plettenberg, A., Mertenskotter, T., Eggers, C., Stellbrink, H.J., 1998. Highly active antiretroviral therapy significantly improves the prognosis of patients with HIV-associated progressive multifocal leukoencephalopathy. Aids 12 (10), 1149–1154.

Amemiya, K., Traub, R., Durham, L., Major, E.O., 1989. Interaction of a nuclear factor-1-like protein with the regulatory region of the human *Polyomavirus* JC virus. J. Biol. Chem. 264 (12), 7025–7032.

Ariza, A., Mate, J.L., Isamat, M., Calatrava, A., Fernandez-Vasalo, A., Navas-Palacios, J.J., 1998. Overexpression of Ki-67 and cyclins A and B1 in JC virus-infected cells of progressive multifocal leukoencephalopathy. J. Neuropathol. Exp. Neurol. 57 (3), 226–230.

Benson, C., White, J., De Bono, J., O'Donnell, A., Raynaud, F., Cruickshank, C., McGrath, H., Walton, M., Workman, P., Kaye, S., Cassidy, J., Gianella-Borradori, A., Judson, I., Twelves, C., 2007. A phase I trial of the selective oral cyclin-dependent kinase inhibitor seliciclib (CYC202; R-Roscovitine), administered twice daily for 7 days every 21 days. Br. J. Cancer 96 (1), 29–37.

Bresnahan, W.A., Boldogh, I., Chi, P., Thompson, E.A., Albrecht, T., 1997. Inhibition of cellular Cdk2 activity blocks human cytomegalovirus replication. Virology 231 (2), 239–247.

Canduri, F., Uchoa, H.B., de Azevedo Jr., W.F., 2004. Molecular models of cyclin-dependent kinase 1 complexed with inhibitors. Biochem. Biophys. Res. Commun. 324 (2), 661–666.

Collazos, J., Mayo, J., Martinez, E., Blanco, M.S., 1999. Contrast-enhancing progressive multifocal leukoencephalopathy as an immune reconstitution event in AIDS patients. Aids 13 (11), 1426–1428.

Davido, D.J., Leib, D.A., Schaffer, P.A., 2002. The cyclin-dependent kinase inhibitor roscovitine inhibits the transactivating activity and alters the posttranslational modification of herpes simplex virus type 1 ICP0. J. Virol. 76 (3), 1077–1088.

De Azevedo, W.F., Leclerc, S., Meijer, L., Havlicek, L., Strnad, M., Kim, S.H., 1997. Inhibition of cyclin-dependent kinases by purine analogues: crystal structure of human cdk2 complexed with roscovitine. Eur. J. Biochem. 243 (1–2), 518–526.

Elphick, G.F., Querbes, W., Jordan, J.A., Gee, G.V., Eash, S., Manley, K., Dugan, A., Stanifer, M., Bhatnagar, A., Kroeze, W.K., Roth, B.L., Atwood, W.J., 2004. The human *Polyomavirus*, JCV, uses serotonin receptors to infect cells. Science 306 (5700), 1380–1383.

Endo, S., Okada, Y., Orba, Y., Nishihara, H., Tanaka, S., Nagashima, K., Sawa, H., 2003. JC virus agnoprotein colocalizes with tubulin. J. Neurovirology 9 (Suppl 1), 10–14.

Habran, L., Bontems, S., Di Valentin, E., Sadzot-Delvaux, C., Piette, J., 2005. Varicella-zoster virus IE63 protein phosphorylation by roscovitine-sensitive cyclin-dependent kinases modulates its cellular localization and activity. J. Biol. Chem. 280 (32), 29135–29143.

Hall, C.D., Dafni, U., Simpson, D., Clifford, D., Wetherill, P.E., Cohen, B., McArthur, J., Hollander, H., Yainnoutsos, C., Major, E., Millar, L., Timpone, J., 1998. Failure of cytarabine in progressive multifocal leukoencephalopathy associated with human immunodeficiency virus infection. AIDS Clinical Trials Group 243 Team. N. Engl. J. Med. 338 (19), 1345–1351.

Hirt, B., 1967. Selective extraction of polyoma DNA from infected mouse cell cultures. J. Mol. Biol. 26 (2), 365–369.

Kerr, D., Chang, C.F., Chen, N., Gallia, G., Raj, G., Schwartz, B., Khalili, K., 1994. Transcription of a human neurotropic virus promoter in glial cells: effect of YB-1 on expression of the JC virus late gene. J. Virol. 68 (11), 7637–7643.

Kim, R.J., Moine, S., Reese, D.K., Bullock, P.A., 2002. Peptides containing cyclin/Cdk-nuclear localization signal motifs derived from viral initiator proteins bind to DNA when unphosphorylated. J. Virol. 76 (23), 11785–11792.

Komagome, R., Sawa, H., Suzuki, T., Suzuki, Y., Tanaka, S., Atwood, W.J., Nagashima, K., 2002. Oligosaccharides as receptors for JC virus. J. Virol. 76 (24), 12992–13000.

Kudoh, A., Daikoku, T., Sugaya, Y., Isomura, H., Fujita, M., Kiyono, T., Nishiyama, Y., Tsurumi, T., 2004. Inhibition of S-phase cyclin-dependent kinase activity blocks expression of Epstein–Barr virus immediate-early and early genes, preventing viral lytic replication. J. Virol. 78 (1), 104–115.

Marra, C.M., Rajicic, N., Barker, D.E., Cohen, B.A., Clifford, D., Donovan Post, M.J., Ruiz, A., Bowen, B.C., Huang, M.L., Queen-Baker, J., Andersen, J., Kelly, S., Shriver, S., 2002. A pilot study of cidofovir for progressive multifocal leukoencephalopathy in AIDS. Aids 16 (13), 1791–1797.

McClue, S.J., Blake, D., Clarke, R., Cowan, A., Cummings, L., Fischer, P.M., MacKenzie, M., Melville, J., Stewart, K., Wang, S., Zhelev, N., Zheleva, D., Lane, D.P., 2002. In vitro and in vivo antitumor properties of the cyclin dependent kinase inhibitor CYC202 (R-roscovitine). Int. J. Cancer 102 (5), 463–468.

McVey, D., Brizuela, L., Mohr, I., Marshak, D.R., Gluzman, Y., Beach, D., 1989. Phosphorylation of large tumour antigen by cdc2 stimulates SV40 DNA replication. Nature 341 (6242), 503–507.

McVey, D., Ray, S., Gluzman, Y., Berger, L., Wildeman, A.G., Marshak, D.R., Tegtmeyer, P., 1993. cdc2 phosphorylation of threonine 124 activates the origin-unwinding functions of simian virus 40 T antigen. J. Virol. 67, 5206–5215.

McVey, D., Woelker, B., Tegtmeyer, P., 1996. Mechanisms of simian virus 40 T-antigen activation by phosphorylation of threonine 124. J. Virol. 70 (6), 3887–3893.

Meijer, L., Borgne, A., Mulner, O., Chong, J.P., Blow, J.J., Inagaki, N., Inagaki, M., Delcros, J.G., Moulinoux, J.P., 1997. Biochemical and cellular effects of roscovitine, a potent and selective inhibitor of the cyclin-dependent kinases cdc2, cdk2 and cdk5. Eur. J. Biochem. 243 (1–2), 527–536.

Moarefi, I.F., Small, D., Gilbert, I., Hopfner, M., Randall, S.K., Schneider, C., Russo, A., Ramsperger, U., Arthur, A.K., Stahl, H., et al., 1993. Mutation of the cyclin-dependent kinase phosphorylation site in simian virus 40 (SV40) large T antigen specifically blocks SV40 origin DNA unwinding. J. Virol. 67 (8), 4992–5002.

Nukuzuma, S., Yogo, Y., Guo, J., Nukuzuma, C., Itoh, S., Shinohara, T., Nagashima, K., 1995. Establishment and characterization of a carrier cell culture producing high titres of polyoma JC virus. J. Med. Virol. 47 (4), 370–377.

Okada, Y., Sawa, H., Tanaka, S., Takada, A., Suzuki, S., Hasegawa, H., Umemura, T., Fujisawa, J., Tanaka, Y., Hall, W.W., Nagashima, K., 2000. Transcriptional activation of JC virus by human T-lymphotropic virus type I Tax protein in human neuronal cell lines. J. Biol. Chem. 275 (22), 17016–17023.

Okada, Y., Sawa, H., Endo, S., Orba, Y., Umemura, T., Nishihara, H., Stan, A.C., Tanaka, S., Takahashi, H., Nagashima, K., 2002. Expression of JC virus agnoprotein in progressive multifocal leukoencephalopathy brain. Acta Neuropathol. (Berl.) 104 (2), 130–136.

Orba, Y., Sawa, H., Iwata, H., Tanaka, S., Nagashima, K., 2004. Inhibition of virus production in JC virus-infected cells by postinfection RNA interference. J. Virol. 78 (13), 7270–7273.

Radhakrishnan, S., Gordon, J., Del Valle, L., Cui, J., Khalili, K., 2004. Intracellular approach for blocking JC virus gene expression by using RNA interference during viral infection. J. Virol. 78 (13), 7264–7269.

Ranganathan, P.N., Khalili, K., 1993. The transcriptional enhancer element, kappa B, regulates promoter activity of the human neurotropic virus, JCV, in cells derived from the CNS. Nucleic Acids Res. 21 (8), 1959–1964.

Raynaud, F.I., Whittaker, S.R., Fischer, P.M., McClue, S., Walton, M.I., Barrie,

S.E., Garrett, M.D., Rogers, P., Clarke, S.J., Kelland, L.R., Valenti, M., Brunton, L., Eccles, S., Lane, D.P., Workman, P., 2005. In vitro and in vivo pharmacokinetic-pharmacodynamic relationships for the trisubstituted aminopurine cyclin-dependent kinase inhibitors olomoucine, bohemine and CYC202. Clin. Cancer Res. 11 (13), 4875–4887.

Ruffini, F., Arbour, N., Blain, M., Olivier, A., Antel, J.P., 2004. Distinctive properties of human adult brain-derived myelin progenitor cells. Am. J. Pathol. 165 (6), 2167–2175.

Sadowska, B., Barrucco, R., Khalili, K., Safak, M., 2003. Regulation of human *Polyomavirus* JC virus gene transcription by AP-1 in glial cells. J. Virol. 77 (1), 665–672.

Sanchez, V., Spector, D.H., 2006. Cyclin-dependent kinase activity is required for efficient expression and posttranslational modification of human cytomegalovirus proteins and for production of extracellular particles. J. Virol. 80 (12), 5886–5896.

Sanchez, V., McElroy, A.K., Yen, J., Tamrakar, S., Clark, C.L., Schwartz, R.A., Spector, D.H., 2004. Cyclin-dependent kinase activity is required at early times for accurate processing and accumulation of the human cytomegalovirus UL122-123 and UL37 immediate-early transcripts and at later times for virus production. J. Virol. 78 (20), 11219–11232.

Schang, L.M., 2002. Cyclin-dependent kinases as cellular targets for antiviral drugs. J. Antimicrob. Chemother. 50 (6), 779–792.

Schang, L.M., 2004. Effects of pharmacological cyclin-dependent kinase inhibitors on viral transcription and replication. Biochim. Biophys. Acta 1697 (1–2), 197–209.

Schang, L.M., Phillips, J., Schaffer, P.A., 1998. Requirement for cellular cyclin-dependent kinases in herpes simplex virus replication and transcription. J. Virol. 72 (7), 5626–5637.

Schang, L.M., Rosenberg, A., Schaffer, P.A., 1999. Transcription of herpes simplex virus immediate-early and early genes is inhibited by roscovitine, an inhibitor specific for cellular cyclin-dependent kinases. J. Virol. 73 (3), 2161–2172.

Schang, L.M., Bantly, A., Knockaert, M., Shaheen, F., Meijer, L., Malim, M.H., Gray, N.S., Schaffer, P.A., 2002. Pharmacological cyclin-dependent kinase inhibitors inhibit replication of wild-type and drug-resistant strains of herpes simplex virus and human immunodeficiency virus type 1 by targeting cellular, not viral, proteins. J. Virol. 76 (15), 7874–7882.

Suzuki, S., Sawa, H., Komagome, R., Orba, Y., Yamada, M., Okada, Y., Ishida, Y., Nishihara, H., Tanaka, S., Nagashima, K., 2001. Broad distribution of the JC virus receptor contrasts with a marked cellular restriction of virus replication. Virology 286 (1), 100–112.

Swenson, J.J., Frisque, R.J., 1995. Biochemical characterization and localization of JC virus large T antigen phosphorylation domains. Virology 212 (2), 295–308.

Swenson, J.J., Trowbridge, P.W., Frisque, R.J., 1996. Replication activity of JC virus large T antigen phosphorylation and zinc finger domain mutants. J. Neurovirology 2 (2), 78–86.

Taylor, S.L., Kinchington, P.R., Brooks, A., Moffat, J.F., 2004. Roscovitine, a cyclin-dependent kinase inhibitor, prevents replication of varicella-zoster virus. J. Virol. 78 (6), 2853–2862.

Vita, M., Abdel-Rehim, M., Olofsson, S., Hassan, Z., Meurling, L., Siden, A., Siden, M., Pettersson, T., Hassan, M., 2005. Tissue distribution, pharmacokinetics and identification of roscovitine metabolites in rat. Eur. J. Pharm. Sci. 25 (1), 91–103.

Wang, D., de la Fuente, C., Deng, L., Wang, L., Zilberman, I., Eadie, C., Healey, M., Stein, D., Denny, T., Harrison, L.E., Meijer, L., Kashanchi, F., 2001. Inhibition of human immunodeficiency virus type 1 transcription by chemical cyclin-dependent kinase inhibitors. J. Virol. 75 (16), 7266–7279.

Wegner, M., Drolet, D.W., Rosenfeld, M.G., 1993. Regulation of JC virus by the POU-domain transcription factor Tst-1: implications for progressive multifocal leukoencephalopathy. Proc. Natl. Acad. Sci. U. S. A. 90 (10), 4743–4747.

Wroblewska, Z., Wellish, M., Gilden, D., 1980. Growth of JC virus in adult human brain cell cultures. Arch. Virol. 65 (2), 141–148.

Transgenic expression of *Helicobacter pylori* CagA induces gastrointestinal and hematopoietic neoplasms in mouse

Naomi Ohnishi*, Hitomi Yuasa*, Shinya Tanaka†, Hirofumi Sawa‡, Motohiro Miura*, Atsushi Matsui*, Hideaki Higashi*, Manabu Musashi§, Kazuya Iwabuchi¶, Misao Suzuki‖, Gen Yamada‖, Takeshi Azuma**, and Masanori Hatakeyama*††

*Division of Molecular Oncology, Institute for Genetic Medicine and Division of Chemistry, Graduate School of Science, §Health Administration Center, and ¶Division of Immunobiology, Institute for Genetic Medicine, Hokkaido University, Sapporo 060-0815, Japan; †Laboratory of Molecular and Cellular Pathology, Hokkaido University Graduate School of Medicine, Sapporo 060-8638, Japan; ‡Department of Molecular Pathobiology, Hokkaido University Research Center for Zoonosis Control, Sapporo 001-0020, Japan; ‖Center for Animal Resources and Development, Graduate School of Medical and Pharmaceutical Sciences, Kumamoto University, Kumamoto 860-0811, Japan; and **Department of Gastroenterology, Kobe University Graduate School of Medicine, Kobe 650-0017, Japan

Communicated by Tadatsugu Taniguchi, University of Tokyo, Tokyo, Japan, November 27, 2007 (received for review October 26, 2007)

Infection with *cagA*-positive *Helicobacter pylori* is associated with gastric adenocarcinoma and gastric mucosa-associated lymphoid tissue (MALT) lymphoma of B cell origin. The *cagA*-encoded CagA protein is delivered into gastric epithelial cells via the bacterial type IV secretion system and, upon tyrosine phosphorylation by Src family kinases, specifically binds to and aberrantly activates SHP-2 tyrosine phosphatase, a bona fide oncoprotein in human malignancies. CagA also elicits junctional and polarity defects in epithelial cells by interacting with and inhibiting partitioning-defective 1 (PAR1)/microtubule affinity-regulating kinase (MARK) independently of CagA tyrosine phosphorylation. Despite these CagA activities that contribute to neoplastic transformation, a causal link between CagA and *in vivo* oncogenesis remains unknown. Here, we generated transgenic mice expressing wild-type or phosphorylation-resistant CagA throughout the body or predominantly in the stomach. Wild-type CagA transgenic mice showed gastric epithelial hyperplasia and some of the mice developed gastric polyps and adenocarcinomas of the stomach and small intestine. Systemic expression of wild-type CagA further induced leukocytosis with IL-3/GM-CSF hypersensitivity and some mice developed myeloid leukemias and B cell lymphomas, the hematological malignancies also caused by gain-of-function SHP-2 mutations. Such pathological abnormalities were not observed in transgenic mice expressing phosphorylation-resistant CagA. These results provide first direct evidence for the role of CagA as a bacterium-derived oncoprotein (bacterial oncoprotein) that acts in mammals and further indicate the importance of CagA tyrosine phosphorylation, which enables CagA to deregulate SHP-2, in the development of *H. pylori*-associated neoplasms.

bacterial oncoprotein | transgenic mouse

Gastric adenocarcinoma is the fourth most common cancer and second leading cause of cancer-related death worldwide (1). Infection with *Helicobacter pylori* is the strongest risk factor for the development of gastric adenocarcinoma (2). *H. pylori* infection is also associated with mucosa-associated lymphoid tissue (MALT) lymphoma of B cell origin (3). *H. pylori is* subdivided into *cagA*-positive and *cagA*-negative strains and the *cagA*-positive strains are much more potent in induction of mucosal damage and severe atrophic gastritis (4, 5). Furthermore, epidemiological studies have suggested a critical role of *cagA*-positive *H. pylori* in the development of gastric adenocarcinoma (6, 7). The *cagA*-encoded CagA protein is delivered into gastric epithelial cells via the bacterial type IV secretion system (8), where it undergoes tyrosine phosphorylation by Src or Abl kinase at the Glu-Pro-Ile-Tyr-Ala (EPIYA) motifs present in variable numbers in the C-terminal region (9–12). Tyrosine-phosphorylated CagA then specifically binds to and aberrantly activates SHP-2 tyrosine phosphatase (9, 14), a bona fide oncoprotein whose gain-of-function mutations are associated with human malignancies (13). CagA-deregulated SHP-2 perturbs the Erk MAP kinase (15) and also dephosphorylates focal adhesion kinase (FAK) to induce an elongated cell-shape known as the hummingbird phenotype (8, 16). In addition, CagA interacts with Grb2 and c-Met in a phosphorylation-independent manner (17, 18) and Crk in a phosphorylation-dependent manner (19), which may have additional roles in the morphogenetic activity of CagA. More recently, CagA was found to impair the cell–cell interaction independently of CagA tyrosine phosphorylation. CagA disrupts tight junctions and causes the loss of apical-basolateral polarity in polarized epithelial cells by binding and inhibiting partitioning-defective 1 (PAR1)/microtubule affinity-regulating kinase (MARK) (20). CagA also destabilizes the E-cadherin/β-catenin complex, a major component of the adherens junctions, and thereby deregulates the β-catenin signal (21). Because normal epithelial architecture constrains abnormal cell proliferation (22), its disorganization by CagA may also contribute neoplastic transformation of cells.

Despite accumulating *in vitro* evidence for the transforming potential of CagA, the exact role of CagA in *in vivo* tumorigenesis remains obscure. Infection of wild-type mice with *H. pylori* does not result in the development of gastric carcinoma, probably because of poor host adaptation. Whereas long-term infection with *H. pylori* can induce gastric carcinoma in Mongolian gerbils, it remains uncertain whether CagA plays an active role in carcinogenesis in gerbils (23–25). Accordingly, rodent models have so far failed to demonstrate a causal link between CagA and the development of neoplasms *in vivo*.

In this work, we generated CagA transgenic mice and found that CagA induces abnormal proliferation of gastric epithelial cells and hematopoietic cells, followed by the development of gastrointestinal carcinomas and leukemias/lymphomas, in a tyrosine phosphorylation-dependent manner. Our findings reveal that *H. pylori* CagA is the first bacterial oncoprotein that acts in mammals.

Results

Synthesis and Analysis of the Humanized *cagA* Gene. Due to the structural polymorphism in the EPIYA-repeat region, individual CagA species show differential degrees of SHP-2-binding activity, which influences the magnitude of CagA virulence (8). We re-

Author contributions: M.H. designed research; N.O., H.Y., M. Miura, A.M., H.H., M. Musashi, and K.I. performed research; M.S., G.Y., and T.A. contributed new reagents/analytic tools; S.T. and H.S. analyzed data; and N.O., H.Y., M. Miura, A.M., H.H., and M.H. wrote the paper.

The authors declare no conflict of interest.

††To whom correspondence should be addressed. E-mail: mhata@igm.hokudai.ac.jp.

This article contains supporting information online at www.pnas.org/cgi/content/full/0711183105/DC1.

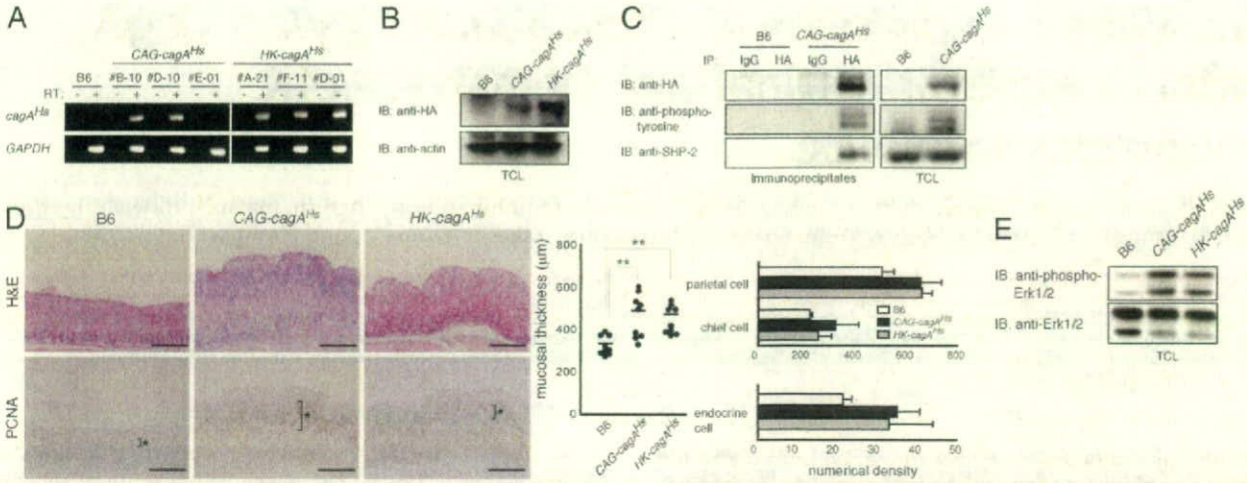

Fig. 1. Establishment of CagA transgenic mice. (*A*) $cagA^{Hs}$ mRNAs in the stomachs of 4-week-old $cagA^{Hs}$ heterozygous male mice as determined by RT-PCR. B6, C57BL/6J; RT, reverse transcription. *GAPDH* was used as a control. (*B*) Immunoblot analysis of CagA expression in the stomachs of 12-week-old B6, *CAG-cagA*^{Hs} (B-10), and *HK-cagA*^{Hs} (F-11) heterozygous male mice. IB, immunoblotting; TCL, total cell lysates. (*C*) Expression, tyrosine phosphorylation, and SHP-2-complex formation of CagA in embryonic fibroblasts prepared from B6 or *CAG-cagA*^{Hs} heterozygous mice (B-10). IP, immunoprecipitation. (*D*) Histological analysis of the glandular stomachs from 12-week-old B6, *CAG-cagA*^{Hs} (B-10), and *HK-cagA*^{Hs} (A-21) heterozygous male mice. *, PCNA-labeled cells. (Scale bars, 300 μm.) Mucosal thickness in the glandular stomach and numerical density of epithelial cells per millimeter of gastric mucosal height in these mice are shown. **, $P < 0.05$, Student's *t* test. Error bars indicate mean ± SD of triplicates. (*E*) Immunoblot analysis of Erk phosphorylation in gastric hyperplasia developed in $cagA^{Hs}$ mice.

ported that a CagA species possessing two repeated EPIYA-D segments (ABDD CagA) exhibits the greatest ability to bind and activate SHP-2 (26). Accordingly, we chose a *cagA* gene encoding ABDD CagA as the transgene in mice. The *H. pylori*-derived *cagA* gene is characterized by A/T-rich sequences, which could induce rapid gene silencing after integration into mammalian genomes [supporting information (SI) Fig. 5]. Also, *cagA* contains multiple ATTTA sequences that act as mRNA degradation motifs in mammalian cells (27). To avoid these potential problems, we chemically synthesized a DNA fragment encoding the entire ORF (3,729 base pairs) of ABDD CagA while converting bacterial *cagA* codons to those more commonly used in human genes, which significantly reduced the A/T contents and eliminated the ATTTA sequence (SI Fig. 5*B*). The synthesized DNA was then 3′-tagged with a sequence encoding the hemagglutinin (HA) to generate the humanized *cagA* gene ($cagA^{Hs}$). Expectedly, transfection of a $cagA^{Hs}$ expression vector gave rise to higher levels of CagA expression and greater magnitude for induction of cells with the hummingbird phenotype than did a bacterial *cagA* vector in AGS human gastric epithelial cells (SI Fig. 6).

Generation of Transgenic Mice Bearing Humanized *cagA* Gene. To express CagA systemically in mice, $cagA^{Hs}$ was connected downstream of the chicken β-*actin* and *globin* fusion promoter (*CAG* promoter) (28). The $cagA^{Hs}$ DNA was also connected downstream of the β *subunit* gene promoter of mouse H^+/K^+-*ATPase* (*HK* promoter) (29), with the expectation of predominant expression of CagA in the stomach (SI Fig. 7*A*). After injection of the transgenic constructs into fertilized mouse eggs, three lines (B-10, D-10, and E-01) of the *CAG* promoter-driven $cagA^{Hs}$ (*CAG-cagA*^{Hs}) transgenic mice and three lines (A-21, F-11, and D-01) of the *HK* promoter-driven $cagA^{Hs}$ (*HK-cagA*^{Hs}) transgenic mice were established (SI Fig. 7*B*). These $cagA^{Hs}$ mice were indistinguishable from the wild-type littermates in behavior and weight when they were born, and they developed normally. No overt difference was found between $cagA^{Hs}$ heterozygous and homozygous mice.

In *CAG-cagA*^{Hs} mice, $cagA^{Hs}$ mRNAs were detected in various organs and tissues with high levels of expression in the stomach, ileum, colon, brain, lung, thymus, and testis (Fig. 1*A* and SI Fig. 8*A*). In *HK-cagA*^{Hs} mice, $cagA^{Hs}$ mRNAs were predominantly expressed in the stomach. However, significant amounts of $cagA^{Hs}$ transcripts were also present in other tissues such as the lung, intestine, thymus, spleen, and testis, indicating leaky transcription from the transgenic *HK* promoter (Fig. 1*A* and SI Fig. 8 *A* and *B*). Expression of the CagA protein was confirmed in tissue extracts prepared from the stomachs of 4-week-old *CAG-cagA*^{Hs} and *HK-cagA*^{Hs} transgenic mice (Fig. 1*B*), although the levels were much lower than those of gastric epithelial cells transfected with CagA-expression vector or *in vitro* infected with *cagA*-positive *H. pylori* (data not shown). Analysis of embryonic fibroblasts from *CAG-cagA*^{Hs} mice confirmed tyrosine phosphorylation of CagA and complex formation of CagA with SHP-2 (Fig. 1*C*).

Gastrointestinal Abnormalities in Wild-type CagA Transgenic Mice. At 12 weeks of age, mice were killed and autopsies revealed a broad thickening of gastric mucosa, primarily at the body of the stomach, in both the *CAG-cagA*^{Hs} and *HK-cagA*^{Hs} mice, although the penetrance of this mucosal change was incomplete (Fig. 1*D* and SI Fig. 9). This may be attributable to the differences in CagA levels among individual transgenic mice even though they are genetically identical. Histologically, the change was due to epithelial hyperplasia of the glandular stomach, in which the proliferative zone in the gastric gland was markedly expanded, and was concomitantly associated with increased numbers of parietal, chief, and endocrine cells, which were all derived from precursors present in the proliferative zone (Fig. 1*D*). In the hyperplastic lesion, CagA expression was concomitantly associated with the hyperactivation of the Erk MAP kinase, a downstream effector of CagA-deregulated SHP-2 (Fig. 1*E*) (15).

At 48 weeks of age, several *CAG-cagA*^{Hs} and *HK-cagA*^{Hs} mice had developed polyps in the glandular stomach. These polyps were mostly hyperplastic polyps, consisting of surface epithelial cells with limited atypical cellularity without nuclear pseudostratification. By 72 weeks of age, 15 of 184 *CAG-cagA*^{Hs}/line B-10 mice, 8 of 35 *CAG-cagA*^{Hs}/line D-10 mice and 5 of 98 *HK-cagA*^{Hs}/line A-21 mice had developed hyperplastic polyps (Fig. 2*A* and SI Table 1). Furthermore, a small number of $cagA^{Hs}$ mice at 72 weeks of age had developed adenocarcinomas, two in the stomach and four in the small intestine (five in *CAG-cagA*^{Hs}/line B-10 and 1 in *HK-cagA*^{Hs}/line F-11) (Fig. 2 *B* and *C* and SI Table 1). These

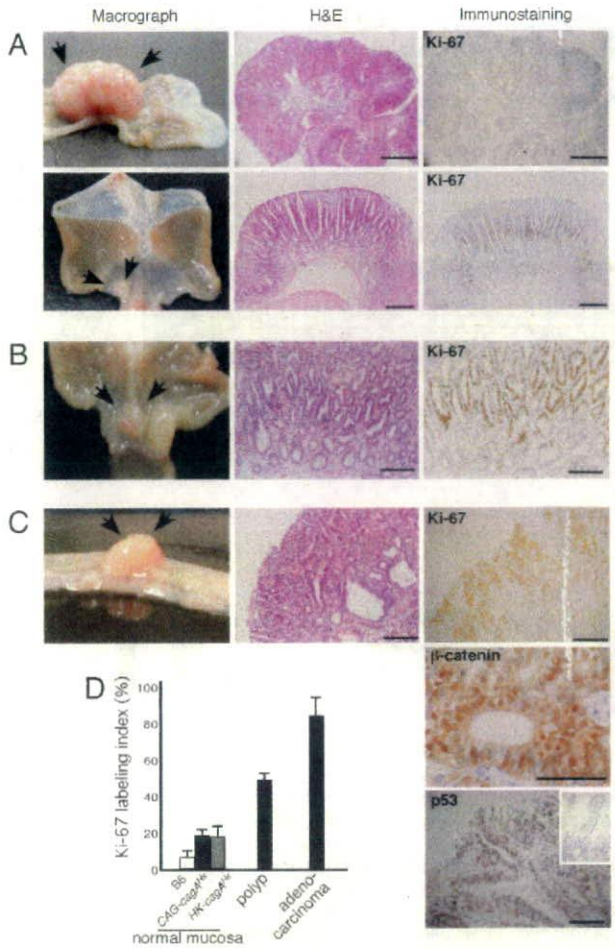

Fig. 2. Gastrointestinal polyps and adenocarcinomas in *cagA*^{Hs} mice. Histological analysis of H&E staining and immunostaining. (*A*) Hyperplastic polyps developed in the stomachs of 72-week-old *CAG-cagA*^{Hs} (B-10) homozygous female mice (*Upper*) and *HK-cagA*^{Hs} (A-21) heterozygous male (*Lower*) mice. Scale bars, 300 μm. (*B*) Adenocarcinoma developed in the stomach of a 72-week-old *CAG-cagA*^{Hs} homozygous male mouse (B-10). Scale bars, 100 μm. (*C*) Adenocarcinoma developed in the small intestine of a 72-week-old *CAG-cagA*^{Hs} heterozygous male mouse (B-10). In the p53-immunostaining panel, matched control is shown in *Inset*. (Scale bars, 100 μm.) (*D*) Ki-67 labeling indexes of gastric lesions in *cagA*^{Hs} mice. Error bars indicate mean ± SD.

carcinomas consisted of irregular branching glands lined by atypical columnar cells that showed plump nuclei with large nucleoli and high mitotic index (SI Fig. 10*A*). The high proliferating activity of the tumors was confirmed by Ki-67 immunostaining (Fig. 2 *C* and *D*). In several cases, neoplastic glands had penetrated the lumina muscularis mucosa (SI Fig. 10*B*). Immunostaining of the tumor specimens demonstrated intense nuclear positivity of p53 and β-catenin in intestinal adenocarcinomas, suggesting mutations in the *β-catenin* and/or *Apc* and *p53* genes in the neoplastic lesions but not in gastric adenocarcinomas (Fig. 2*C* and data not shown). These findings indicate the requirement of cell type-specific secondary events for the development of gastrointestinal neoplasms. No gastrointestinal polyps or tumors were found in the wild-type littermate mice by 72 weeks after birth with continual observation (n = 100).

It has been generally believed that atrophic gastritis and intestinal metaplasia, a transdifferentiation of gastric epithelial cells to an intestinal phenotype, are precancerous gastric mucosal changes, from which intestinal-type gastric adenocarcinoma arises (30). We therefore performed histological examination of gastric mucosa from 72-week-old *cagA*^{Hs} mice but did not find any signs of pathological abnormalities (data not shown). From these observations, we concluded that CagA has the ability to induce epithelial hyperplasia, polyps, and adenocarcinomas in the stomach, without causing overt inflammation or intestinal metaplasia. We also note that no overt histopathological abnormalities were found in the intestinal tract of *cagA*^{Hs} mice without tumors.

Hematopoietic Abnormalities in Wild-Type CagA Transgenic Mice. In addition to the gastrointestinal abnormalities, some of the *cagA*^{Hs} mice had developed hematopoietic malignancies by 72 weeks of age (16 of 152 in *CAG-cagA*^{Hs}/line B-10; 1 of 77 in *HK-cagA*^{Hs}/line A-21; and 1 of 38 in *HK-cagA*^{Hs}/line F-11) (SI Table 1). It should be noted here that CagA was also expressed in the spleen of *HK-cagA*^{Hs} mice (SI Fig. 8*B*). The leukemic mice showed marked splenomegaly, and immunohistochemical analyses of the spleens revealed that they were of myeloid (5 cases), B cell (12 cases), or T cell (1 case) origin (Fig. 3 *A–C*). Mild leukocytosis (granulocytosis) was also found in the peripheral blood of 72-week-old *cagA*^{Hs} mice without hematological malignancies (Fig. 3*D*). No age-matched wild-type littermate mice developed hematological abnormality (n = 100).

The observed spectrum of hematological malignancies in CagA transgenic mice was similar to that evoked by gain-of-function SHP-2 mutations (13). We thus suspected that CagA-deregulated SHP-2 is also involved in the transformation of hematopoietic cells as well. Indeed, in spleen cells from *cagA*^{Hs} mice, the Erk MAP kinase was again hyperactivated (Fig. 3*E*). Because SHP-2 potentiates cellular responses to interleukin (IL)-3 and granulocyte-macrophage colony-stimulating factor (GM-CSF) (31), we performed a colony assay to evaluate activation status of SHP-2. Bone marrow cells from *cagA*^{Hs} mice showed hypersensitivity to IL-3 and GM-CSF and also exhibited spontaneous colony formation in the absence of cytokines (Fig. 3*F*). These observations are consistent with the idea that SHP-2 is deregulated in *cagA*^{Hs} mice and suggest that CagA-deregulated SHP-2 plays a key role in the abnormal proliferation of multiple hematopoietic cells.

Role of Tyrosine Phosphorylation in the *in Vivo* Pathogenic Activity of CagA. Tyrosine-phosphorylated CagA specifically binds to and deregulates SHP-2. To explore the role of CagA tyrosine phosphorylation in the development of gastrointestinal and hematopoietic lesions observed in *cagA*^{Hs} mice, we next generated a *PR-cagA*^{Hs} gene encoding a phosphorylation-resistant ABDD CagA (PR-CagA), which cannot bind SHP-2, from *cagA*^{Hs} (SI Fig. 11 *A* and *B*). Transgenic constructs were made by connecting the *PR-cagA*^{Hs} DNA fragment downstream of the *CAG* or *HK* promoter (SI Fig. 11*C*). After injection of the transgenic constructs into fertilized mouse eggs, three lines each for the *CAG* promoter-driven *PR-cagA*^{Hs} (*CAG-PR-cagA*^{Hs}) and *HK* promoter-driven *PR-cagA*^{Hs} (*HK-PR-cagA*^{Hs}) transgenic mice were established (Fig. 4*A*). Systemic expression of *PR-cagA*^{Hs} in *CAG-PR-cagA*^{Hs} mice was confirmed by RT-PCR analysis (SI Fig. 11*D*). Again, expression of *PR-cagA*^{Hs} in *HK-PR-cagA*^{Hs} mice was not specific to the stomach.

Despite significantly higher levels of PR-CagA expression than those of wild-type CagA in transgenic mice (Fig. 4 *B* and *C*), *PR-cagA*^{Hs} mice neither showed gastric epithelial hyperplasia or leukocytosis nor developed neoplasms (except one case of gastric hyperplastic polyp in a *HK-PR-cagA*^{Hs} mouse) (Fig. 4 *D* and *E*, SI Fig. 11*E*, and SI Table 1). Furthermore, bone marrow cells from *PR-cagA*^{Hs} mice did not show hypersensitivity to IL-3 or GM-CSF (Fig. 4*F*). These observations indicate that tyrosine-phosphorylated CagA, which enables CagA to bind SHP-2, plays an important role in the abnormal proliferation of gastric epithelial and hematopoietic cells and subsequent development of neoplasms.

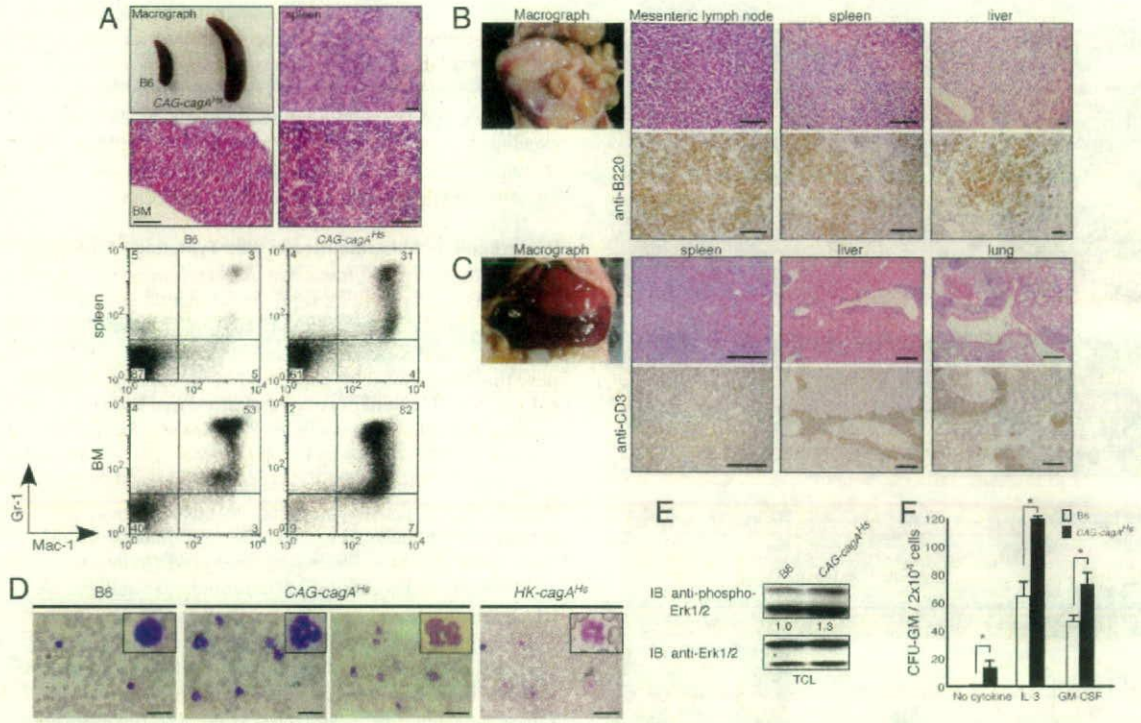

Fig. 3. Hematological abnormalities in *cagA*^{Hs} mice. (*A*) Myeloid leukemia developed in a 72-week-old *CAG-cagA*^{Hs} heterozygous male mouse (B-10). (*Upper*) Macroscopic and histological views of the spleen and bone marrow (BM) from the mouse with leukemia. Age-matched control B6 spleen is also shown. (Scale bars, 100 μm.) (*Lower*) FACS analyses of spleen and BM cells from the mice with leukemias. Cells were double-stained with anti-Gr-1 and anti-Mac-1 antibodies, showing increased numbers of Mac-1/Gr-1-double-positive myeloid cells. The percentage of each cell population is indicated. BM cells from B6 mice were used as a control. (*B*) B cell lymphoma of mesenteric lymph-node origin developed in a 72-week-old *CAG-cagA*^{Hs} (B-10) heterozygous male mice. Macroscopic view, H&E staining, and anti-B220 immunostaining showing diffuse infiltration of B cells into the spleen and liver, resembling diffuse large B cell lymphoma. (Scale bars, 100 μm.) (*C*) T cell lymphoma developed in a 72-week-old *CAG-cagA*^{Hs} (B-10) homozygous male mice. Macroscopic view, H&E staining and anti-CD3 immunostaining showing infiltration of T cells into the spleen, liver, and lung. (Scale bars, 300 μm.) (*D*) Blood smears from 72-week-old B6, *CAG-cagA*^{Hs} (B-10) and *HK-cagA*^{Hs} (F-11) heterozygous male mice, showing increased granulocytes in *cagA*^{Hs} mice. (Scale bars, 30 μm.) (*E*) Immunoblot analysis of Erk phosphorylation in spleen cells from B6 or *CAG-cagA*^{Hs} (B-10) mice. (*F*) Myeloid colonies derived from bone marrow cells of 72-week-old B6 or *CAG-cagA*^{Hs} (B-10) heterozygous male mice with no evidence of hematopoietic malignancies. Error bars indicate mean ± SD of triplicates. *, $P < 0.05$, Student's *t* test.

Discussion

In this work, we generated CagA transgenic mice in which involvement of other bacterial factors in pathogenesis is totally excluded, and we obtained formal evidence that CagA is a bacterial oncoprotein, the expression of which suffices for development of neoplasms. Despite systemic expression in mice, CagA exhibits oncogenic actions specifically toward gastrointestinal and hematopoietic cells. Because the tumor formation depends on CagA tyrosine phosphorylation, the observed tissue-specific oncogenic action of CagA might reflect the differential activation status of CagA kinases, such as Src and Abl, in different cell lineages. Furthermore, given that CagA tyrosine phosphorylation is an essential prerequisite for the interaction of CagA with SHP-2 oncoprotein (9, 14), our results point to the importance of CagA-deregulated SHP-2 in *in vivo* tumorigenesis.

SHP-2 is required for normal development of both myeloid and lymphoid lineage cells (32, 33), and gain-of-function mutations of SHP-2 are associated with childhood leukemias (13, 33, 34). We found in this work that bone marrow cells from *cagA*^{Hs} mice exhibit hypersensitivity to IL-3 and GM-CSF, the hallmark of SHP-2 activation (31, 35). The finding provides evidence for the hyperactivation of SHP-2 in *cagA*^{Hs} mice and suggests the role of CagA-deregulated SHP-2 in leukemogenesis. This in turn raises the possibility that CagA is also involved in the development of *H. pylori*-associated B cell MALT lymphoma, although the association of *cagA*-positive *H. pylori* with MALT lymphoma is still controversial (3, 4, 36). It would be interesting to know whether CagA can be delivered into B cells that migrate to the *H. pylori*-infected stomach.

Whereas *cagA*^{Hs} mice develop both gastrointestinal and hematopoietic malignancies, SHP-2 mutation is rarely found in solid tumors (37). Also, notably, mice systemically expressing a gain-of-function SHP-2 mutant developed myeloproliferative disease but not solid tumors (35). These observations suggest that development of gastrointestinal tumors in *cagA*^{Hs} mice, which still depends on CagA tyrosine phosphorylation, requires additional CagA activities that cooperate with CagA-deregulated SHP-2. An intriguing idea is that phosphorylation-independent interaction of CagA with PAR1, which inhibits PAR1 kinase activity and thereby causes junctional and polarity defects in epithelial cells (20), is also involved the development of solid tumors. Indeed, the connection between epithelial cell polarity and tumors has been provided by the works of *Drosophila* tumor suppressor genes such as *dlg*, *lgl*, and *scribble* (22, 38). Also notably, PAR1 is a downstream target of LKB1/PAR4 kinase, loss-of-function mutations of which lead to the gastrointestinal cancer-prone Peutz–Jeghers syndrome (39).

The rare and delayed appearance of neoplasms in *cagA*^{Hs} mice indicates a weak oncogenic potential of CagA quantitatively and/or qualitatively. Nevertheless, the efficiency of tumors developed among different strains of *cagA*^{Hs} mice was still correlated with the levels of CagA expressed. Notably, expression of wild-type CagA was significantly lower than that of PR-CagA in transgenic mice, possibly because robust activation of SHP-2 by high levels of

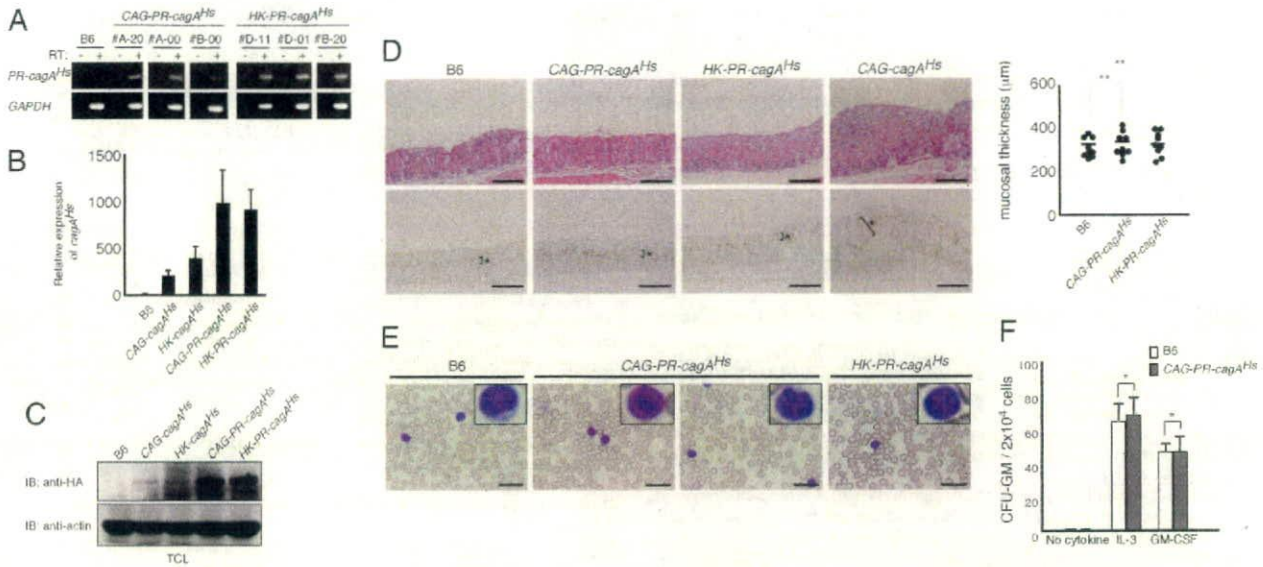

Fig. 4. Analysis of transgenic mice expressing phospho-resistant (PR) CagA. (*A*) *PR-cagA*^{Hs} mRNAs in the stomachs of 12-week-old *PR-cagA*^{Hs} heterozygous male mice as determined by RT-PCR analysis. (*B*) Relative *cagA*^{Hs} mRNA levels in the stomachs of 12-week-old B6, *CAG-cagA*^{Hs} (B-10), *HK-cagA*^{Hs} (A-21), *CAG-PR-cagA*^{Hs} (A-20), and *HK-PR-cagA*^{Hs} (D-01) heterozygous male mice. Error bars indicate mean ± SD of triplicates. (*C*) Immunoblot analysis of CagA expression in the stomachs of 12-week-old B6, *CAG-cagA*^{Hs} (B-10), *HK-cagA*^{Hs} (A-21), *CAG-PR-cagA*^{Hs} (A-20), and *HK-PR-cagA*^{Hs} (D-01) heterozygous male mice. (*D*) H&E staining and anti-PCNA immunostaining of the glandular stomachs from 12-week-old B6, *CAG-PR-cagA*^{Hs} (A-20), *HK-PR-cagA*^{Hs} (D-01), and *CAG-cagA*^{Hs} (B-10) heterozygous male mice. *, PCNA-labeled cells. (Scale bars, 300 μm.) Gastric mucosal thicknesses of these mice are shown at *Right*. **, $P > 0.05$, Student's *t* test. (*E*) Blood smears from 72-week-old B6, *CAG-PR-cagA*^{Hs} (A-20), and *HK-PR-cagA*^{Hs} (B-20) heterozygous male mice. (*F*) Myeloid colonies derived from bone marrow cells of 72-week-old B6 or *CAG-PR-cagA*^{Hs} (A-20) heterozygous male mice with no evidence of hematopoietic malignancies. Error bars indicate mean ± SD of triplicates. *, $P > 0.05$, Student's *t* test.

wild-type CagA is not tolerated during embryogenesis as suggested (35). Such a quantitative restriction on wild-type CagA expression could explain at least in part the low incidence of neoplasms in *cagA*^{Hs} mice. Intriguingly, *cagA*^{Hs} mice develop gastric epithelial hyperplasia and tumors in the absence of overt mucosal inflammation or metaplastic change. This finding suggests that the oncogenic potential of CagA is cell-autonomous and that development of gastric carcinoma does not necessarily require chronic inflammation and presumed precancerous conditions, such as intestinal metaplasia. Obviously, however, the notion does not exclude the possibility that host responses to *H. pylori* infection, such as production of a variety of inflammatory cytokines, potentiate the weak oncogenic activity of CagA. It is also possible that low levels of CagA elicits gastric epithelial cell proliferation, whereas high levels of CagA triggers apoptosis, possibly by inducing oncogenic stress as described (14–16).

Once established, maintenance of the transformed phenotype of gastric adenocarcinoma no longer requires CagA. Hence, whereas CagA plays a critical role during the early steps of gastric carcinogenesis, populations of preneoplastic cells that undergo continuous CagA exposure may progress to spawn cell variants that acquire additional oncogenic changes, such as those involved in the SHP-2/Ras/Erk pathway, and/or apoptotic regulation, such as p53, as shown in the CagA-induced intestinal carcinoma, which compensate CagA functions and thereby confer CagA-independence during the later phases of carcinogenesis.

Our study establishes a causal relationship between *H. pylori* CagA and tumorigenesis and suggests that CagA is a critical molecular target for therapeutic application to *H. pylori*-associated neoplasms.

Materials and Methods

Transgenic Mice. Chemically synthesized *cagA*^{Hs} DNA was subcloned into pCAGGS (28) or pHKATP vector (29). The *CAG-cagA*^{Hs} or *HK-cagA*^{Hs} fragment consisting of the promoter, *cagA*^{Hs} and polyA cassettes derived from β-*globin* gene was excised from the resulting plasmid by restriction enzyme digestion, and then injected directly into fertilized eggs of C57BL/6J mice. Transgenic mice were identified by PCR analysis of tail DNAs, using *cagA*^{Hs}-specific primers (*cagA*^{Hs}-forward 5′-CACAATAACGCTCTGTCATCAGTGCTG-3′, *cagA*^{Hs}-reverse 5′-TCAACGTATAAGACACTTCCCCATTGC-3′). PCR amplification was performed at 94°C for 5 min, 94°C for 30 seconds, 62°C for 30 seconds, 72°C for 30 seconds (30 cycles), and 72°C for 7 min. All of the animal experiments were carried out according to the protocol approved by the Ethics Committee for Animal Experiments at Hokkaido University.

RT-PCR and Quantitative RT-PCR. Total RNA was extracted from mouse tissues with the use of TRIzol Reagent (Invitrogen). Quantitative RT-PCR was performed by using SYBR Green fluorescence detection system (Qiagen) with ABI PRISM 7700 sequencer (Applied Biosystems). The following primer pairs were used for PCR amplification: *cagA*^{Hs}-forward: 5′-AAGCTGCTTCTGCGATTAACCG-3′, *cagA*^{Hs}-reverse: 5′-GGAGTCTTTCAGTTCGTC-3′, *GAPDH*-forward: 5′-ACCACAGTCCATGCCATCAC-3′, and *GAPDH*-reverse: 5′-TCCACCACCCTGTTGCTGTA-3′.

Immunoprecipitation and Immunoblotting. Protein extracts prepared from tissues or cells were subjected to immunoprecipitation or immunoblotting with an anti-HA antibody (3F10; Roche) as described in ref. 9.

Histopathological Analyses. Tissue specimens were fixed in formalin, embedded in paraffin, sectioned, and stained with hematoxylin and eosin (H&E). Thickness of gastric mucosa was evaluated by measuring three distinct points of the glandular stomach for each mouse. Cancer diagnosis was made based on Ki-67 labeling index, nuclear atypia, and mitosis counts by two independent pathologists (S.T. and H.S.). For immunohistochemical staining, sections were deparaffinized, rehydrated, and then incubated with anti-PCNA (PC10; Dako), anti-Ki-67 (Dako), anti-B220 (RA3–6B2), anti-p53 (CM5; Novocastra), anti-CD3 (Dako), or anti-β-catenin antibody (BD Bioscience). Sections were then washed and incubated with appropriate secondary antibodies. Reacted antibodies were detected by the peroxydase reaction, using diaminobenzidine as substrate. Chief cells were identified by H&E staining. Parietal cells and endocrine cells were identified by immunostaining with anti-H^+/K^+-ATPase α-subunit antibody (Chemicon) and anti- chromogranin A antibody (Dako), respectively. Peripheral blood smears were stained with May–Giemsa solution.

Flow Cytometry. Cells were washed in PBS containing 0.5% BSA and 0.05% NaN_3. Fc receptor-mediated binding was blocked by preincubation of cells with supernatants of 2.4G2 hybridoma. Fluorescence isothiocyanate (FITC)-anti-Gr-1 and phycoerythrin (PE)-anti-CD11b (Mac-1) antibodies were purchased from BD Bioscience. Flow cytometric analysis was performed by using FACSCalibur (Becton–Dickinson) and analyzed with CellQuest software.

Colony Assay. Methylcellulose cell culture was performed in 35-mm culture dishes as described in ref. 40.

Statistical Analysis. Statistical analysis was performed by using Student's *t* test, the χ^2 test, or Fisher's exact test.

ACKNOWLEDGMENTS. We thank J. I. Gordon for pHKATP-hGH1, K. Shimizu and Y. Shibuta for technical assistance, and K. Nagashima and S. Kon for advice. This work was supported by Grants-in-Aid for Scientific Research from the Ministry of Education, Culture, Sports, Science and Technology of Japan and by a Takeda Science Foundation Research Grant (to M.H.). N.O. is a Japan Society for the Promotion of Science Research Fellow.

1. Parkin DM (2001) Global cancer statistics in the year 2000. *Lancet Oncol* 2:533–543.
2. Peek RM, Jr, Blaser MJ (2002) *Helicobacter pylori* and gastrointestinal tract adenocarcinomas. *Nat Rev Cancer* 2:28–37.
3. Parsonnet J, *et al.* (1994) *Helicobacter pylori* infection and gastric lymphoma. *N Engl J Med* 330:1267–1271.
4. Kuipers EJ, Perez-Perez GI, Meuwissen SG, Blaser MJ (1995) *Helicobacter pylori* and atrophic gastritis: importance of the *cagA* status. *J Natl Cancer Inst* 87:1777–1780.
5. Sozzi M, *et al.* (1998) Atrophic gastritis and intestinal metaplasia in *Helicobacter pylori* infection: the role of CagA status. *Am J Gastroenterol* 93:375–379.
6. Blaser MJ, *et al.* (1995) Infection with *Helicobacter pylori* strains possessing *cagA* is associated with an increased risk of developing adenocarcinoma of the stomach. *Cancer Res* 55:2111–2115.
7. Parsonnet J, Friedman GD, Orentreich N, Vogelman H (1997) Risk for gastric cancer in people with CagA positive or CagA negative *Helicobacter pylori* infection. *Gut* 40:297–301.
8. Segal ED, Cha J, Lo J, Falkow S, Tompkins LS (1999) Altered states: Involvement of phosphorylated CagA in the induction of host cellular growth changes by *Helicobacter pylori*. *Proc Natl Acad Sci USA* 96:14559–14564.
9. Higashi H, *et al.* (2002) SHP-2 tyrosine phosphatase as an intracellular target of *Helicobacter pylori* CagA protein. *Science* 295:683–686.
10. Higashi H, *et al.* (2002) Biological activity of the *Helicobacter pylori* virulence factor CagA is determined by variation in the tyrosine phosphorylation sites. *Proc Natl Acad Sci USA* 99:14428–14433.
11. Selbach M, Moese S, Hauck CR, Meyer TF, Backert S (2002) Src is the kinase of the *Helicobacter pylori* CagA protein *in vitro* and *in vivo*. *J Biol Chem* 277:6775–6778.
12. Poppe M, Feller SM, Römer G, Wessler S (2007) Phosphorylation of *Helicobacter pylori* CagA by c-Abl leads to cell motility. *Oncogene* 26:3462–3472.
13. Tartaglia M, Gelb BD (2005) Germ-line and somatic *PTPN11* mutations in human disease. *Eur J Med Genet* 48:81–96.
14. Hatakeyama M (2004) Oncogenic mechanisms of the *Helicobacter pylori* CagA protein. *Nat Rev Cancer* 4:688–694.
15. Higashi H, *et al.* (2004) *Helicobacter pylori* CagA induces Ras-independent morphogenetic response through SHP-2 recruitment and activation. *J Biol Chem* 279:17205–17216.
16. Tsutsumi R, Takahashi A, Azuma T, Higashi H, Hatakeyama M (2006) Focal adhesion kinase is a substrate and downstream effector of SHP-2 complexed with *Helicobacter pylori* CagA. *Mol Cell Biol* 26:261–276.
17. Churin Y, *et al.* (2003) *Helicobacter pylori* CagA protein targets the c-Met receptor and enhances the motogenic response. *J Cell Biol* 161:249–255.
18. Mimuro H, *et al.* (2002) Grb2 is a key mediator of *Helicobacter pylori* CagA protein activities. *Mol Cell* 10:745–755.
19. Suzuki M, *et al.* (2005) Interaction of CagA with Crk plays an important role in *Helicobacter pylori*-induced loss of gastric epithelial cell adhesion. *J Exp Med* 202:1235–1247.
20. Saadat I, *et al.* (2007) *Helicobacter pylori* CagA targets PAR1/MARK kinase to disrupt epithelial cell polarity. *Nature* 447:330–333.
21. Murata-Kamiya N, *et al.* (2007) *Helicobacter pylori* CagA interacts with E-cadherin and deregulates the β-catenin signal that promotes intestinal transdifferentiation in gastric epithelial cells. *Oncogene* 26:4617–4626.
22. Bilder D (2004) Epithelial polarity and proliferation control: links from the *Drosophila* neoplastic tumor suppressors. *Genes Dev* 18:1909–1925.
23. Honda S, *et al.* (1998) Development of *Helicobacter pylori*-induced gastric carcinoma in Mongolian gerbils. *Cancer Res* 58:4255–4259.
24. Watanabe T, Tada M, Nagai H, Sasaki S, Nakao M (1998) *Helicobacter pylori* infection induces gastric cancer in Mongolian gerbils. *Gastroenterology* 115:642–648.
25. Rieder G, Merchant JL, Haas R (2005) *Helicobacter pylori* cag-type IV secretion system facilitates corpus colonization to induce precancerous conditions in Mongolian gerbils. *Gastroenterology* 128:1229–1242.
26. Naito M, *et al.* (2006) Influence of EPIYA-repeat polymorphism on the phosphorylation-dependent biological activity of *Helicobacter pylori* CagA. *Gastroenterology* 130:1181–1190.
27. Ross J (1996) Control of messenger RNA stability in higher eukaryotes. *Trends Genet* 12:171–175.
28. Araki K, Araki M, Miyazaki J, Vassalli P (1995) Site-specific recombination of a transgene in fertilized eggs by transient expression of Cre recombinase. *Proc Natl Acad Sci USA* 92:160–164.
29. Lorenz RG, Gordon JI (1993) Use of transgenic mice to study regulation of gene expression in the parietal cell linage of gastric units. *J Biol Chem* 268:26559–26570.
30. Correa P (1992) Human gastric carcinogenesis: a multistep and multifactorial process–First American Cancer Society Award Lecture on Cancer Epidemiology and Prevention. *Cancer Res* 52:6735–6740.
31. Schubbert S, *et al.* (2005) Functional analysis of leukemia-associated *PTPN11* mutations in primary hematopoietic cells. *Blood* 106:311–317.
32. Qu CK, *et al.* (1997) A deletion mutation in the SH2-N domain of Shp-2 severely suppresses hematopoietic cell development. *Mol Cell Biol* 17:5499–5507.
33. Qu CK, Nguyen S, Chen J, Feng GS (2001) Requirement of Shp-2 tyrosine pohosphatase in lymphoid and hematopoietic cell development. *Blood* 97:911–914.
34. Tartaglia M, *et al.* (2003) Somatic mutations in *PTPN11* in juvenile myelomonocytic leukemia, myelodysplastic syndromes and acute myeloid leukemia. *Nat Genet* 34:148–150.
35. Araki T, *et al* (2004) Mouse model of Noonan syndrome reveals cell type- and gene dosage-dependent effects of *Ptpn11* mutation. *Nat Med* 10:849–857.
36. De Jong D, *et al.* (1996) Gastric non-Hodgkin lymphomas of mucosa-associated lymphoid tissue are not associated with more aggressive *Helicobacter pylori* strains as identified by CagA. *Am J Clin Pathol* 106:670–675.
37. Bentires-Alj M, *et al.* (2004) Activating mutations of the noonan syndrome-associated *SHP2/PTPN11* gene in human solid tumors and adult acute myelogenous leukemia. *Cancer Res* 64:8816–8820.
38. Humbert P, Russell S, Richardson H (2003) Dlg, Scribble and Lgl in cell polarity, cell proliferation and cancer. *Bioessays* 25:542–553.
39. Alessi DR, Sakamoto K, Bayascas JR (2006) LKB1-dependent signaling pathways. *Annu Rev Biochem* 75:137–163.
40. Musashi M, *et al.* (1991) Phorbol ester enhancement of IL-3-dependent proliferation of primitive hematopoietic progenitors of mice. *J Pharmacol Exp Ther* 280:225–231.